Mechanisms of diabetes mellitus-associated depletion of interstitial cells of Cajal in the murine stomach

Viktor J. Horváth, M.D.

1st Department of Internal Medicine
University of Szeged

Ph.D. Thesis

2008

This thesis is based on the following publications:

I, **Ördög T, Redelman D, Miller LJ, Horváth VJ, Zhong Q, Almeida-Porada G, Zanjani ED, Horowitz B, Sanders KM.** Purification of interstitial cells of Cajal by fluorescence-activated cell sorting. *Am J Physiol Cell Physiol* 286:C448–C456, 2004

II, **Horvath VJ, Vittal H, Ordog T.** Reduced insulin and IGF-I signaling, not hyperglycemia, underlies the diabetes-associated depletion of interstitial cells of Cajal in the murine stomach. *Diabetes* 54:1528-33, 2005.

III, **Horváth VJ, Vittal H, Lőrincz A, Chen H, Almeida-Porada G, Redelman D, Ördög T.** Reduced stem cell factor links smooth myopathy and loss of interstitial cells of Cajal in murine diabetic gastroparesis. *Gastroenterology* 130:759-770, 2006.

Abbreviations:

ICC: interstitial cells of Cajal

SCF: stem cell factor

IGF-I: insulin-like growth factor-I

igf1r: insulin-like growth factor-I receptor

insr: insulin receptor

FACS: fluorescence-activated cell sorting

FCM: flowcytometry

NOD: non-obese diabetic

Contents

Acknowledgement:

I would express my special thanks to Dr. Tamás Ördög for his kind invitation and support to perform of these experiments in the Department of Physiology and Cell Biology, Cellular Imaging Laboratory, University of Nevada, Reno, Nevada.

I would also express my special thanks to Professor Gábor Jancsó for his generous efforts to help me from the beginning of my scientific carreer.

I am grateful to Professor János Lonovics and Professor Tibor Wittmann, the previous and present head of the 1st Department of Initernal Medicine of the University of Szeged to support me during my studies.

I also have to express my thanks to the members of the laboratories where the experiments were completed, particularly to Doug Redelman, Ph.D., Dr. Andrea Lőrincz, and Michael R. Bardsley for their help and to my colleagues in the Department of Physiology, Faculty of Medicine, University of Szeged, especially Dr. Péter Sántha and Dr. Mária Dux for their support.

The excellent technical assistance of Nancy Horowitz and Lisa Miller is also appreciated.

I also thank the patience and help of my family and friends that provided me a safe background.

This work was supported in part by NIH grant DK58185.

Introduction

1.1. *Interstitial cells of Cajal: a historical overview and recognition of their functional significance*

A great body of experimental and clinical evidence indicates that the interstitial cells of Cajal (ICC) play an important role in gastrointestinal physiology as crucial determinants of gastrointestinal motility. Ramon Y Cajal, who first described these cells through the use of methylene blue and silver chromate staining (1893), suggested that these cells were primitive neurons (1, 2). Electron microscopy allowed a distinction of ICC from neurons, macrophages and Schwann cells (3), though their true nature and origin remained unclear. Some investigators regarded ICC as specialized smooth muscle cells (4, 5), while others considered them fibroblast-like (6-12). The ICC of the small bowel were classified into four different types on the basis of their myofilament contents (11). In later studies, their morphological features and their connection with smooth muscle cells and nerves suggested that the ICC of the human esophagus and stomach were specialized smooth muscle cells and not connective tissue elements (12). Important however, that in contrast with smooth muscle cells the ICC were observed to be richly endowed with cytoplasmic organelles such as mitochondria but were poor in contractile elements - similar to the pacemaker cells in the heart. These findings were considered to support the notion previously proposed by Tiegs (13) that ICC may be responsible for the origin and conduction of the rhythmic activity of the gastrointestinal smooth muscle and could serve as pacemaker cells throughout the alimentary canal (12).

Researchers who set out to describe the anatomy and identify the role played by ICC had the disadvantage of not possessing a specific marker for labeling these cells in their environment and distinguishing them from other cell types similar in their appearance to ICC. The development of immunohistochemical techniques and the availability of highly specific antibodies opened up new possibilities for the discovery of a specific marker for the labeling of ICC. In the 1990s several research groups recognized that ICC express the gene product of the proto-oncogene c-*kit* that encodes the type III receptor tyrosine

kinase, Kit (15-18), which is located in the *white spotting* (*W*) locus. Labeling of Kit (or in later studies amplification of *c-kit* mRNA) furnished an efficient tool with which to study the morphology and function of this highly specialized cell type throughout the entire gastrointestinal tract of different species, including man, guinea pig, mouse, rat and birds, by using light microscopy. Immunohistochemistry involving the use of c-*kit* labeling has provided a means of investigating the structure and distribution of ICC networks and has improved our understanding of the anatomic relationships among ICC, enteric neurons, smooth muscle cells and other resident cells, such as macrophages in the *tunica muscularis.* With this new technique it became possible to study the role of ICC in pathophysiological conditions, and the changes that the ICC undergo in certain disorders (19). It has emerged that ICC are disrupted in several motility disorders and there is growing evidence that these cells play an essential part in the pathophysiology of human gastrointestinal disorders, such as ulcerative colitis (20), achalasia (22), Chagas` disease (21) and diabetic gastroparesis (25, 26). It has also been demonstrated that gastrointestinal stromal tumors may originate from c-*kit*-positive cells (23). Another important advance in the recognition of the c-*kit* positivity of ICC was the realization that cell signaling via c-*kit* receptor is essential for the development and maintenance of ICC networks (16, 18). Block c-*kit* function with neutralizing antibodies (*e.g.* ACK2, the antibody most commonly used in ICC research) impaired the development of ICC (16), and several studies have revealed that animals carrying non-lethal mutations in c-*kit* (18, 27) or stem cell factor (SCF or steel factor, 27, 28), the natural ligand for c-*kit*, have defects in ICC networks. Experiments on these animal models, which lack specific populations of ICC, but do not appear to have neural or smooth muscle defects, have provided important insight into the function and pathophysiological significance of ICC.

1.2. *Morphology and function of the ICC*

Through the c-*kit* positivity of the gastrointestinal ICC, evidence has been acquired for a pacemaker role of ICC in producing contractions of the gastrointestinal muscles of the stomach, small intestine and colon (40). Although these cells account for only about 5 % of the total cell number of the *tunica muscularis* layer, they play an important role in the

gastrointestinal physiology. With the use of specific c-*kit* antibodies (ACK2, 2b8) against the cells building up the gastrointestinal *tunica muscularis* layer several types of network-forming Cajal cells can be distinguished. ICC can be classified according to their shape or localization within the muscle layers (anatomical classification) but their primary function also allows the distinction of certain ICC subtypes (functional classification). In the region of myenteric plexus (between the circular and longitudinal muscle layers), multipolar ICC form a two-dimensional network with variable density. These cells in the myenteric region generally referred to as IC-MY are the dominant pacemaker cells, although other ICC classes can also contribute to the pacemaker function (35). IC-MY and ICC in submucosal region (IC-SM) form extensive networks within pacemaker regions. These cells also extend into the bulk of the muscle layers in the septa that divide bundles of smooth muscle cells. Thus, pacemaker activity is not necessarily confined to the myenteric and submucosal pacemaker regions, but these pacemakers are dominant in intact muscles. Pacemaking by ICC depends on cycling of Ca^{2+} between intracellular compartments (endoplasmic reticulum and mitochondria) mediated by specialized channels and pumps (29, 30) and rhythmic electrical activity *per se* is the consequence of periodic openings of voltage-insensitive, nonselective cation channels driven by the intracellular Ca^{2+} oscillations (30, 31). Other investigators have suggested a role for Ca^{2+}-regulated Cl^- channels in pacemaker activity (30, 33). Fine processes of pacemaker ICC are interconnected via gap junctions, and electric connections are also made with neighboring smooth muscle cells. Thus, electric events occurring in ICC may be conducted to smooth muscle cells. Simultaneous recordings of electric activity from IC-MY and nearby smooth muscle cells have demonstrated that electric activity occurs first in IC-MY and then it initiates electric responses in the smooth muscle cells (34). Connections between ICC are necessary for the regenerative propagation of slow waves, and extension of ICC networks into the septa between muscle bundles may provide propagation pathways for transmission of slow waves through the tunica muscularis (perhaps analogous to the Purkinje fibers in the heart).

Other types of ICC occur throughout the thicknesses of phasic and tonic muscles of the gastrointestinal tract. These spindle-shaped or elongated ICC are intermingled with the fibers of the circular and longitudinal muscle layers in the esophagus, stomach, colon,

and sphincters. They are referred to as intramuscular ICC (IC-IM). IC-IM are extensively and closely associated with nerve fibers of the enteric nervous system (27) and form very close (<20 nm) synapse-like contacts with varicose nerve terminals of excitatory and inhibitory motor neurons. Cells with similar characteristics, called IC-DMP, are likely to be specialized types of IC-IM and are found in the region of the deep muscular plexus in the small intestine. IC-IM and IC-DMP are functionally innervated by the fibers of gastric enteric nervous system and mediate a significant proportion of the motor input from the enteric nervous system. By relaying excitatory inputs to the fundus and mediating nitrergic relaxation of the pyloric sphincter (36), intramuscular ICC together with the enteric neurons contribute to the "pressure pump" that regulates gastric emptying of liquids (37). In mutant mice lacking IC-IM, field stimulation of intrinsic neurons in the stomach resulted in greatly reduced postjunctional responses to cholinergic and nitrergic nerve stimulation (18, 39). This type of ICC under the influence of extensive cholinergic stimulation (mediated by M3 muscarinergic receptors) or during passive stretch (mediated by EP3 prostanoid receptors) can even become the dominant pacemakers by entraining slow waves generated by myenteric ICC (41). In contrast, myenteric ICC never mediate neural inputs as IC-IM do, but residual nitrergic neuromuscular neurotransmission occurs in mutant mice where this ICC type is not present (41). This type of ICC has been reported to play a role in vagally mediated mechanoreception (38). This function of ICC is the least known, but clearly involves local enteric (42) and vagal (43) neuronal circuits and prostaglandin release (41), and mechanosensitive ion channels (44) are possibly also essential participants in the vagus mediated mechanoreception.

The different types of ICC in the stomach are shown in Figure 1.

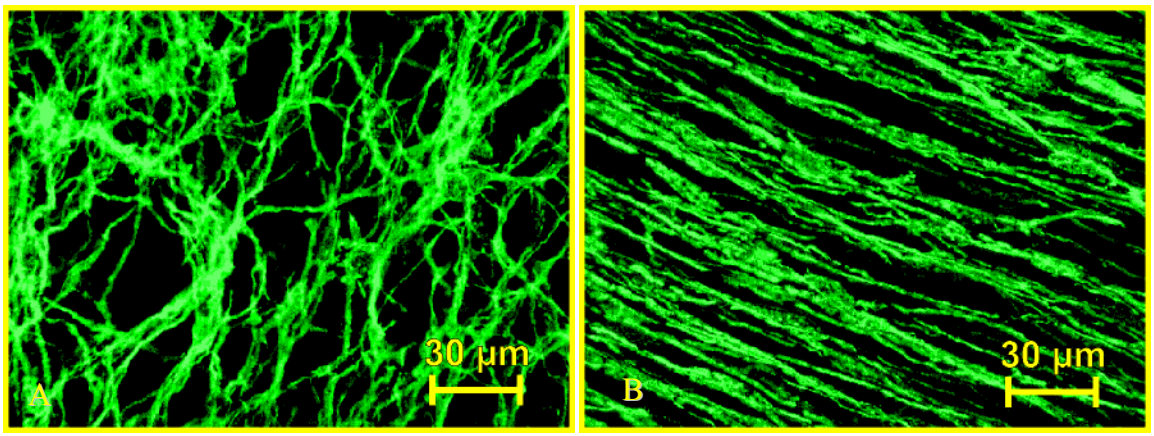

Figure 1. ICC in the murine gastric corpus and antrum. c-*kit* immunohistochemistry. "**A**": representative confocal image of ICC located in the myenteric region of murine antrum (IC-MY). The cells with several processes generate and propagate electrical slow waves. "**B**" representative confocal image of ICC located within the circular and longitudinal muscle layer (IC-IM). Bipolar, spindle-shaped cells mediate neuromuscular neurotransmission.

1.3. *Diabetes-induced changes in gastrointestinal motor functions are associated with an impairment of the Cajal cells*

Diabetic gastropathy, termed broadly as gastric neuromuscular dysfunction, and gastroparesis, defined as symptomatic or asymptomatic gastric retention, occur in up to 50% of patients with type 1 diabetes and 30% of patients with type 2 diabetes (45, 46). The spectrum of symptoms includes postprandial discomfort, bloating, fullness, abdominal pain, and the classic symptoms of gastroparesis: early satiation and recurring nausea and vomiting, which may be self-limiting, recurrent, or unrelenting (45). Asymptomatic gastroparesis may only manifest as poor glycemic control, including hypoglycemia (46). Although diabetic gastropathy is rarely life threatening, it seriously affects the patient's quality of life (45), a prime concern in an aging population.

Normal gastric emptying requires the coordinated work of several cell types, including neurons (both extrinsic and enteric motor neurons), smooth muscle cells and interstitial cells of Cajal. Since pyloric relaxation is dependent on intact nitrergic inhibitory neurons (48, 49) it was understandable that *NOS-/-* knockout mice have delayed gastric emptying (50) and the pharmacological inhibition of NOS can also affect the normal gastric

motility (51, 52). The contribution of ICC to the pathogenesis of gastropathy is also not surprising. It has been clearly proved experimentally that in spontaneously diabetic NOD/LtJ mice, gastroparesis is associated with depletions of networks of ICC in the distal stomach (53). In other studies on human tissues damage to ICC have since been demonstrated in the stomach (54, 55), jejunum (25), and colon (26) of patients with gastroenteropathy due to either type 1 (25) or type 2 (26) diabetes. It has previously also been shown that depletion of pacemaker ICC can result in functional abnormalities (bradygastria, antral tachygastria, arrhythmias, and uncoupling) that are considered hallmarks of diabetic gastroparesis (53, 56, 58). In general, the *tunica muscularis* layer is thicker in diabetic gastropathy than in normal controls and there is evidence that the disruption of protein kinase C activation causes smooth muscle dysfunction (63) in a region specific manner in the human diabetic stomach (64). In human studies, autoantibodies found against smooth muscle L-type Ca^{2+} channel raise the possibility of the contribution of an autoimmune mechanism to diabetic gastroparesis (65).

To prevent or reverse ICC loss in diabetes, it is essential to understand the pathomechanism of this process. Similarly to other long-term complications, chronic or recurring hyperglycemia (47, 60) and resultant oxidative damage, nonenzymatic glycation, and inappropriate activation of protein kinase C, nuclear factor κB, and aldose reductase (59) may play a role. There is also ample evidence that lost (type 1) or reduced and ineffective (type 2) insulin signaling (60, 61), reduced levels of the proinsulin C-peptide (61), and abnormal levels of growth factors, e.g. insulin-like growth factor I (IGF-I) and possibly IGF-II significantly contribute to the pathomechanism of diabetic complications for (61). Indeed, in diabetic mice, infusion of insulin for 1 week has been shown to improve reduced pyloric relaxation and delayed liquid emptying by stimulating neuronal nitric oxide synthesis independent of the concurrent normalization of glucose levels (62). However, ICC depletion and gastroparesis in NOD/LtJ mice occur within 1.5 and 3 months after the onset of diabetes (53), and dissection of the relative significance of hyperglycemia and impaired insulin signaling in chronic *in vivo* studies has been notoriously difficult. For this purpose we developed an organotypic culture model that permits the independent control of insulin, glucose, and growth factor levels over several

months to investigate the mechanism of diabetes-associated ICC depletion in the murine stomach.

1.4. *The aims of the study*

In a murine genetic model of diabetes (35), ICC depletion and gastroparesis occurs within 1.5 and 3 months after the onset of diabetes which means that for the purpose of checking the effects of hyperglycemia and impaired insulin signaling in ICC we needed an *in vitro* approach which allows to be kept intact ICC for months. Accordingly, the first aim of this study was to develop a reliable long-term organotypic culture model for the study of ICC under normal and pathological conditions. With this method our primary aim was the evaluation of the relative significance of hyperglycemia, insulin or IGF-1 signaling in the pathomechanism of diabetes-induced depletion of ICC in murine stomach.
Since these experiments were performed in gastric muscles placed in culture, the effects of insulin and IGF-I may not have been mediated by specific receptors expressed by ICC. Hence, the second aim of the study was to examine whether ICC are direct targets of insulin and IGF-I signaling or whether the effects of these cytokines are mediated by SCF, the only established growth factor for ICC.

Materials and methods

BALB/c mice (9–18 days old) were obtained from breeder pairs purchased from either Simonsen Laboratories (Gilroy, CA), Harlan Sprague-Dawley (Indianapolis, IN) or Charles River Laboratories (Wilmington, MA) or were obtained from our institutional breeding program. BALB/c mice 5–6 wk old were purchased from Charles River or Jackson Laboratories. The animals were anesthetized by isoflurane inhalation (AErrane, Baxter Healthcare, Deerfield, IL) and killed by decapitation. Mice were maintained and the experiments performed in accordance with the National Institutes of Health *Guide for the Care and Use of Laboratory Animals* and the American Physiological Society's "Guiding Principles in the Care and Use of Animals". All protocols were approved by the Institutional Animal Use and Care Committee at the University of Nevada, Reno.

2.1. *Preparation of organotypic cultures*

After decapitation, the stomachs of the juvenile (D9-18) BALB/c mice were removed and the mucosal and submucosal layers were removed by peeling. After the removal of these layers, the intact continuous corpus and antrum *tunica muscularis* tissues (6–7 mg) were pinned, mucosal side up, onto the surface of 35-mm culture dishes coated with Sylgard 184 (Dow Corning, Midland, MI) and incubated at 37 °C in normoglycemic (1 g/l; 5.55 mmol/l) M199 medium (Sigma, St. Louis, MO) containing 2% antibiotic-antimycotic and 2 mmol/l L-glutamine (Invitrogen, Carlsbad, CA). Other supplements (used alone or in combination; see Results) included D-glucose (final concentration: 6 g/l, 33.3 mmol/l, or 10 g/l, 55.5 mmol/l), bovine insulin (5 μg/ml; Cambrex BioScience, Walkersville, MD, or Invitrogen), fetal bovine serum (5%; HyClone, Logan, UT), or murine IGF-I (100 ng/ml; Sigma). All treatments were started within 48 h after establishment of the cultures and maintained throughout the entire experiment. Levels of the supplements were kept constant by changing the culture media every 48 h. This frequency was determined empirically by measuring glucose levels in the spent media with an Accu-Chek Complete blood glucose monitor (Roche Diagnostics, Indianapolis, IN) (57). After 48 h, glucose concentrations did not fall >15 mg/dl (0.8 mmol/l) in the normoglycemic cultures, and no measurable decline could be detected in the hyperglycemic cultures.

2.2. *Immunohistochemistry*

After acetone fixation of the cultured and freshly dissected tissues, ICC were identified with monoclonal (rat) c-*kit* antibodies (ACK2; 5 μg/ml) and Alexa Fluor 488 anti-rat IgG (10 μg/ml; Molecular Probes, Eugene, OR) as previously described (30, 53, 56, 66). Other primary antibodies were used in the experiments: rat IgG2b monoclonal anti-c-Kit clone ACK2 (5 μg/mL), rabbit polyclonal anti-insulin receptor α, anti–IGF-I receptor α, anti-SCF, goat polyclonal anti-insulin receptor α (Santa Cruz Biotechnology; 2 μg/mL), and rabbit polyclonal anti-PGP 9.5 (Biogenesis, Brentwood, NH; 1:200). Secondary antibodies were conjugated with either Alexa Fluor 488, 594, or Texas red (Molecular Probes, Eugene, OR). Live immunolabeling was performed by incubating gastric and

jejunal *tunica muscularis* tissues with antibodies against SCF (2 μg/ml) and neural cell adhesion molecule (CD56; clone: H28.123; 2 μg/ml; Beckman Coulter, Fullerton, CA) at 4°C for 3 hours. Secondary antibodies were applied after fixation with 4% paraformaldehyde-saline. Confocal images of the whole-mounts were taken with a Bio-Rad MRC 600 and a Zeiss LSM 510 META confocal system. To control for the gradients in ICC network densities that occur along both the longitudinal axis and the circumference of the normal murine stomach, images were taken in three representative regions along the greater curve (orad corpus, corpus–antrum border, distal antrum) of each tissue (56). ICC network densities were analyzed quantitatively in superimposed two-dimensional projections of optical sections representing the entire thickness of the whole-mounts by a technique modified from He *et al.* (25) and validated described in a previous study (56). Briefly, cellular and background fluorescence were separated by thresholding on the peak of the distribution of cellular fluorescence. To eliminate variations in brightness within and between images, fluorescence values above and below the threshold were assigned 1 (white) and 0 (black), respectively. ICC densities were expressed as the percent white pixels over a standard area (289 x 193 μm) in the two-dimensional projections and averaged for each tissue (56). Values obtained by this technique are numerical expressions of ICC network densities as they appear in the superimposed confocal sections and neither represent the proportion of ICC nor the fraction of tissue volume occupied by these cells (56).

2.3. *Qualitative and quantitative PCR for the analysis of gene expression*

Quantitative RT-PCR analysis was also performed to assess the c-kit expression in the freshly dissected and cultured murine gastric antrum and corpus tunica muscularis tissue. After the tissue had been cut into small pieces the Trizol (Invitrogen, Carlsbad, CA) method was used to obtain the RNA following the manufacturer's instructions with minor modification. Genomic DNA was removed by incubating total RNA either with RNase-free DNase (5 U per 1 μl per tube; PanVera, Madison, WI) for 20 min at 25 °C, followed by heat inactivation for 5 min at 75 °C, or with the Stratagene Absolutely RNA Nanoprep Kit (La Jolla, CA). Total RNA was reverse transcribed with 200 units of SuperScript II

RNase H$^-$ Reverse Transcriptase (Invitrogen) in a reaction containing 500 ng of oligo d(pT)$_{18}$ primer (New England Biolabs, Beverly, MA), 10 mM of each dNTP, 5x First-Strand Buffer, and 100 mM dithiothreitol (DTT), followed by heat inactivation. The cDNA was amplified with specific primers by using the following protocol: 95 °C for 10 min to activate the Ampli*Taq* polymerase (Applied Biosystems, Foster City, CA), and then 40 or 50 cycles of 95 °C for 15 s and 60 °C for 1 min. Real-time quantitative PCR was performed by using SYBR Green chemistry on a GeneAmp 5700 sequence detector (Applied Biosystems). Standard curves were generated for each primer set by regression analysis of RT-PCRs performed on log$_{10}$-diluted cDNA. Unknown quantities of primers were compared to the housekeeping gene β-actin (GenBank accession no. X03672). Primers were used in the experiments as follows: c-*kit* (Y00864, ICC): sense, nt 2706–2726; antisense, nt 2847–2867; CD68 [NM_009853; macrosialin, a pan-macrophage marker also expressed by some myeloid-derived dendritic cells (68)]: sense, nt 41–65; antisense, nt 201–225; mast cell tryptase (MCT; M57626; mast cells): sense, nt 264–283; antisense, nt 433–454; smooth muscle myosin heavy chain (MyHC; NM_013607; smooth muscle cells): sense, nt 5721–5745; antisense, nt 5930–5954; protein gene product 9.5 (PGP 9.5) or ubiquitin carboxy-terminal hydrolase L1 (a pan-neuronal marker; AF172334): sense, nt 22–44; antisense, nt 171–190; prolyl-4-hydroxylase (BC018411; fibroblasts): sense, nt 1012–1031; antisense, nt 1144–1162, CD34 (NM_133654; fibroblasts, endothelial cells): sense, 109-126; antisense, 280-298, insulin receptor (Insr; NM_010568): sense, 3279-3290; antisense, 3386-3405, IGF-1-receptor (Igf1r; AF056187): sense, 2208-2227; antisense, 2385-2407. Because of alternate mRNA splicing, SCF (*Kitl*, NM_013598) exists in 2 transmembrane forms: the longer one is subject to rapid proteolysis, which gives rise to soluble SCF. The shorter form remains membrane-bound and forms homodimers important for the activation of its receptor, c-Kit. We calculated the expression of the membrane-bound isoform in each sample by subtracting the amount of soluble SCF message (primers: 716–739, 820–843) from the amount of a transcript common to both isoforms (primers: 492–515, 639– 662) (72). All primers were obtained from Keystone Labs (Camarillo, CA). For qualitative analysis the amplified products (10 μl) were separated by electrophoresis on a 2% agarose/1x TAE (Tris, acetic acid, EDTA) gel and the DNA bands were visualized by ethidium bromide

staining. In case of quantitative RT-PCR the transcriptional quantification of gene products was accomplished relative to the ß-actin standard curve and expressed in ß-actin units as transcript per corpus + antrum *tunica muscularis*. To confirm the specificity of the primers, PCR products generated from each pair of primers were extracted and sequenced. We tested for genomic DNA contamination in the source RNA by PCR assay with cytoglobin (AJ315163) primers that span an intron (sense, nt 268–289; antisense, nt 497–519) (68). Nonspecific amplification and spurious primer-dimer fragments were controlled for by omitting the template from the PCR amplification.

2.4. *Analysis of gene expression by hybridization*

Affymetrix (Santa Clara, CA) Mouse Genome 430 2.0 microarrays, which cover the mouse transcriptome (over 39,000 transcripts) on a single array, were used for expression profiling of diabetic and nondiabetic gastric muscles. Total RNA was isolated and purified using Trizol (Invitrogen) and the RNeasy Mini Kit (Qiagen), respectively. RNA was quantified by spectrophotometry and its quality was tested by formaldehyde gel electrophoresis. One-cycle complementary RNA synthesis and hybridization were performed by the Nevada Genomics Center, following the manufacturer's protocols. Chips were scanned with an Affymetrix GeneChip 3000 System. Data were analyzed by using the Affymetrix GeneChip Operating Software and verified by quantitative RT-PCR.

2.5. *Purification of ICC by fluorescence-activated cell sorting (FACS)*

The approach to sort ICC was described previously (69). Briefly, ICC and macrophages in the intact gastric corpus + antrum tunica muscularis were labeled with Alexa Fluor 488- ACK2 and monoclonal phycoerythrin-cyanine 5 (PC5)-anti-F4/80 (Caltag, Burlingame, CA), respectively. After the tissues were dispersed into single-cell suspensions, macrophages and dendritic cells were labeled with superparamagnetic monoclonal antibodies (Miltenyi Biotec, Auburn, CA) against CD11b and CD11c, respectively, and the labeling of macrophages was reinforced with a monoclonal PC5-

anti-CD11b antibody (Caltag). Mast cells and other leukocytes were labeled with monoclonal PC5-anti-CD45 antibodies (eBioscience, San Diego, CA). Macrophages and dendritic cells were then depleted by immunomagnetic selection (Miltenyi). ICC were sorted on either a Beckman Coulter EPICS Elite or a Becton Dickinson (San Jose, CA) FACSVantage instrument. A small aliquot of the 20,000 –100,000 ICC harvested in each experiment was reanalyzed by flow cytometry (FCM) on a Beckman Coulter XL/MCL for purity. Approximately 50,000 cells removed before the immunomagnetic depletion were used as unsorted control.

2.6. *Electrophysiological methods*

The electrical slow-wave activity in cultured and freshly dissected corpus + antrum tissues obtained from 14-day-old mice was analyzed by intracellular recording as described earlier (32, 53, 56,). Transmembrane potential of circular muscle cells impaled with KCl-filled glass microelectrodes was recorded at 37.5 ± 0.5 °C by using an Intra 767 amplifier (World Precision Instruments, Sarasota, FL) and a BIOPAC (Santa Barbara, CA) MP100 data acquisition system.

2.7. *Solutions*

Krebs-Ringer bicarbonate solution contained (in mmol/l) 120.35 NaCl, 5.9 KCl, 2.5 $CaCl_2$, 1.2 $MgCl_2$, 15.5 $NaHCO_3$, 1.2 NaH_2PO_4, and 11.5 glucose, pH 7.3–7.4 when bubbled with 97% O_2 and 3% CO_2. CaPSS contained (in mmol/l) 135 NaCl, 5 KCl, 2 $CaCl_2$, 1.2 $MgCl_2$, 10 glucose, and 10 HEPES, adjusted to pH 7.4 with Tris. CFH contained (in mmol/l) 125 NaCl, 5.36 KCl, 15.5 $NaHCO_3$, 0.336 Na_2HPO_4, 0.44 KH_2PO_4, 10 glucose, 2.9 sucrose, and 11 HEPES, adjusted to pH 7.2 with NaOH. Sorting buffer consisted of CFH containing 2% BSA and 2 mM EDTA.

2.8. *Statistics*

For the purpose of statistical analysis of the sorted cells, SigmaStat statistical software for Windows (version 2.03; SPSS Science, Chicago, IL) was used for all statistical analyses. Data are expressed as means ± SE; *n* signifies the number of tissues in the experiment. In *approach 4*, we used cells pooled from 6 stomachs; therefore, the error bars in Fig. 5b reflect the variability among the triplicates in the assay, and no tests of significance were performed. In the other studies, before tests of significance were performed, data were examined for normality and equal variance to determine whether parametric or nonparametric tests should be employed. The unpaired Student's *t*-test and the Mann-Whitney rank sum test were performed on the raw data. A probability value of $P < 0.05$ was used as a cut-off for statistical significance in all procedure. In tissue culture experiments percentage data were transformed [arcsin(√x)] before statistical analysis. One-way ANOVA or Kruskal-Wallis one-way ANOVA on ranks followed by all-pairwise multiple comparison (Tukey test or Dunn's method, respectively) were used for statistical comparisons.

Results

3.1. *Changes in networks of interstitial cells of Cajal in organotypic cultures*

It has already been proven juvenile corpus + antrum *tunica muscularis* tissue can be cultured for 34 days in unsupplemented normoglycemic media without the detection of any ICC loss (57). Our experiments revealed that using c-*kit*–like immunoreactivity reflecting ICC in the superimposed binarized confocal sections occurred throughout the entire thickness of the whole-mounts occupying 45.5 ± 2.7% of the image area in the freshly dissected controls ($n = 11$) and 37.6 ± 5.1 % in the normoglycemic cultures ($n = 7$; NS). ICC network densities were also not affected under hyperglycemic conditions (33.3 mmol/l for the first 17 days and 55.5 mmol/l for the second 17 days: 44.0 ± 6.0%, $n = 4$; NS). Thus, in the next set of experiments, we extended the culture period to 68–72 days (Figs. 2 and 3). During this prolonged culturing period we detected significant changes in ICC density under both culturing condition relative to freshly dissected

controls. ICC networks (both intramuscular and myenteric) were significantly depleted in the unsupplemented normoglycemic cultures (Figs. 2 and 3, unsupplemented normoglycemic media [NG]). Instead of triggering further depletion of ICC hyperglycemia (55.5 mmol/l throughout the culture period) partially, but significantly, prevented the reduction of both classes of ICC (Figs. 2 and 3, hyperglycemic media [HG]). By the addition of insulin to the culturing media the loss of ICC could be completely prevented. (Figs. 2 and 3, insulin [Ins]), and the networks maintained with the aid of insulin remained unaffected by chronic hyperglycemia (Figs. 2 and 3, hyperglycemic media supplemented with insulin [InsHG]). Measurements of glucose concentrations in 2-day spent media indicated that they were essentially unaffected by tissue utilization. Thus, the lack of effect was not due to a fall of glucose levels by the end of the culture period between media changes. Addition of 5% fetal bovine serum to insulin-supplemented normoglycemic (n = 3) or hyperglycemic (n = 3) media did not influence the results (not shown). IGF-I supplementation mimicked the effects of insulin and completely prevented the depletion of ICC networks under normoglycemic conditions (Figs. 2 and 3, IGF-I).

To confirm our immunohistochemistry data we also assessed ICC cultured for 75 days by using quantitative RT-PCR analysis of c-*kit* expression. The results were similar to those obtained by c-Kit immunohistochemistry: Total c-*kit* expression was significantly reduced in unsupplemented normoglycemic cultures relative to freshly dissected controls (3.0 ± 1.2 ß-actin units, n = 5; controls: 64.7 ± 12.6, n = 8; P = 0.011), and hyperglycemia did not cause a further decrease in c-*kit* mRNA (8.9 ± 5.3, n = 5). Both insulin (n = 5) and IGF-I (n = 5) treatment prevented the reduction seen in the unsupplemented cultures, although the degree of protection varied greatly (insulin 46.2 ± 19.1; IGF-I 70.7 ± 35.1; NS vs. freshly dissected controls).

3.2. *Changes of electrical rhyhmicity in organotypic cultures*

Finally, we examined the effects of hyperglycemia, insulin, and IGF-I on electrical slow-wave activity recorded from circular smooth muscle cells in tissues cultured for 83–86 days (Figs. 4 and 5). In cultures not supplemented with insulin or IGF-I, resting

membrane potentials were depolarized and slow waves could not be recorded, except for a single impalement made in a tissue maintained under hyperglycemia, where arrhythmic activity of very low amplitude was detected. Both insulin and IGF-I prevented depolarization and the loss of slow waves. However, while slow-wave amplitudes were efficiently maintained by either insulin or IGF-I, their frequencies remained at ~50% of those detected in freshly dissected controls, an effect likely caused by culturing *per se* (57). The slower activity was accompanied by a noticeable but statistically insignificant increase in slow-wave duration.

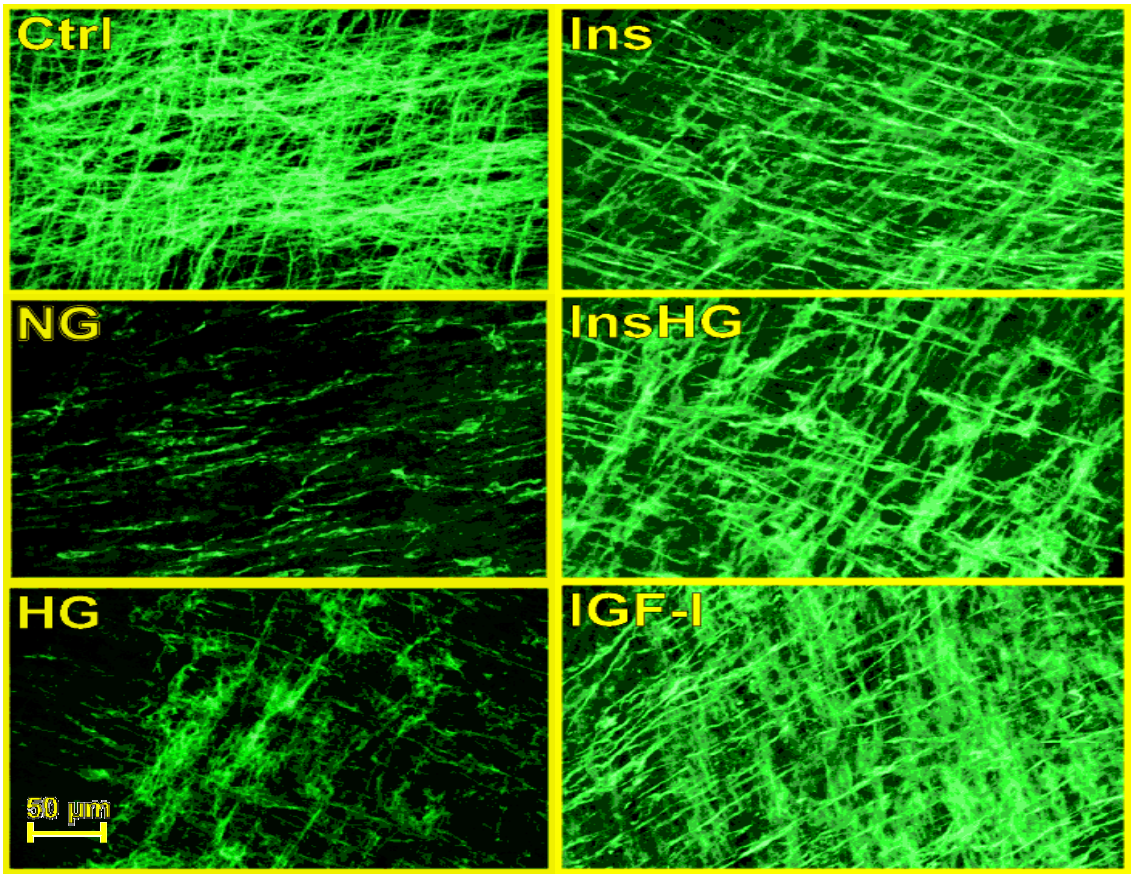

Figure 2. Long-term effects of hyperglycemia, insulin, and IGF-I on ICC networks in organotypic cultures of gastric corpus and antrum tunica muscularis. Representative confocal images of c-Kit–like immunofluorescence in freshly dissected controls (Ctrl) and in tissues cultured for 68–72 days with one or other of the following media are shown: unsupplemented normoglycemic (NG) or hyperglycemic (HG) media, normoglycemic media containing insulin (Ins), hyperglycemic media supplemented with insulin (InsHG), or normoglycemic media containing IGF-I (IGF-I). The images show all ICC that occur within the entire thickness of the tissues projected onto a two-dimensional plane. The scale bar in the bottom left panel applies to all panels.

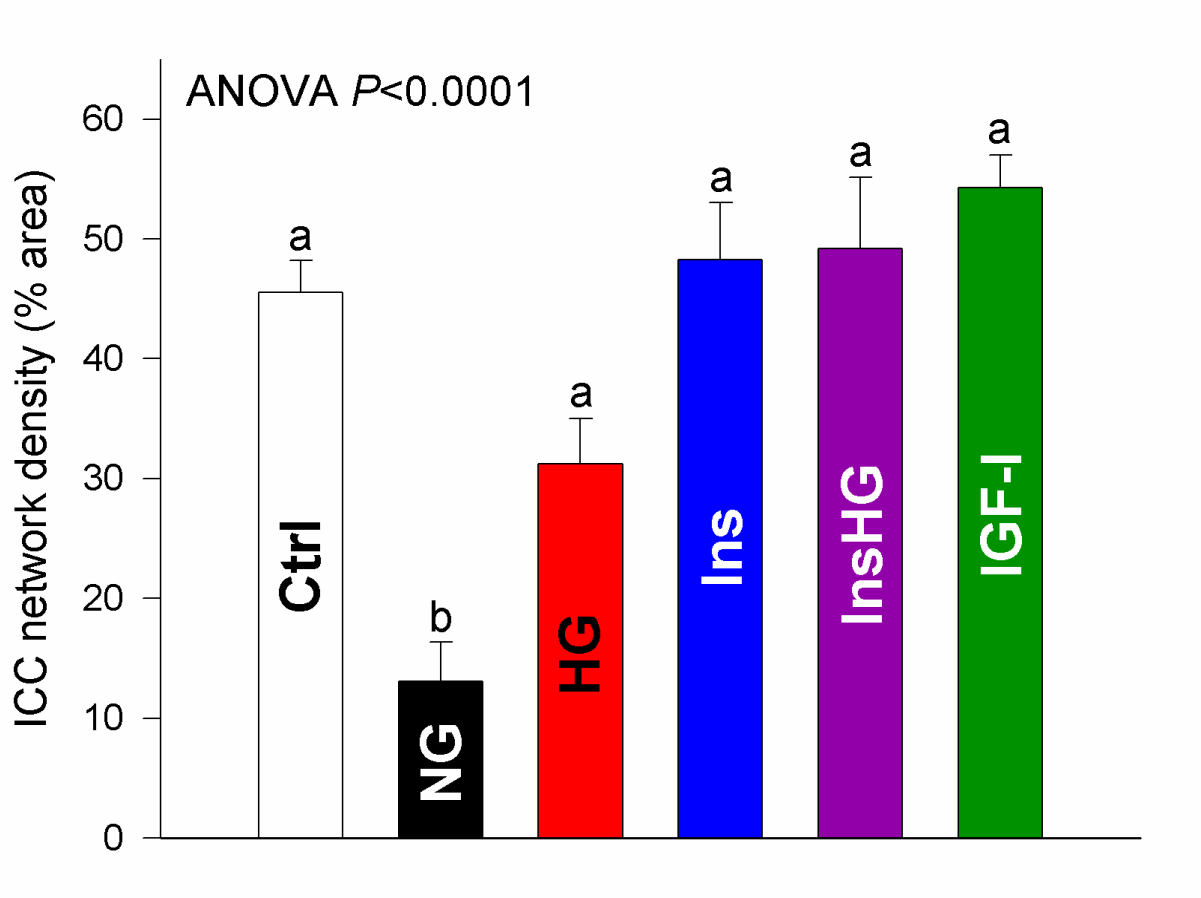

Figure 3. Long-term effects of hyperglycemia, insulin, and IGF-I on ICC networks in organotypic cultures of gastric corpus and antrum tunica muscularis. ICC network densities in the two-dimensional confocal composite images (*e.g.,* those shown in Fig. 2) obtained by quantitative image analysis are shown. Labels correspond to those in Fig. 2. The numbers of cultures in the different treatment groups were as follows: Ctrl: 11, NG: 9, HG: 5, Ins: 8, InsHG: 7, IGF-I: 4. Groups not sharing the same superscript (a or b) are significantly different by multiple comparisons. ICC networks were depleted in long-term unsupplemented normoglycemic cultures, and this reduction could be prevented by insulin (regardless of glucose levels) or IGF-I. Note the partial prevention of ICC loss by high glucose concentrations.

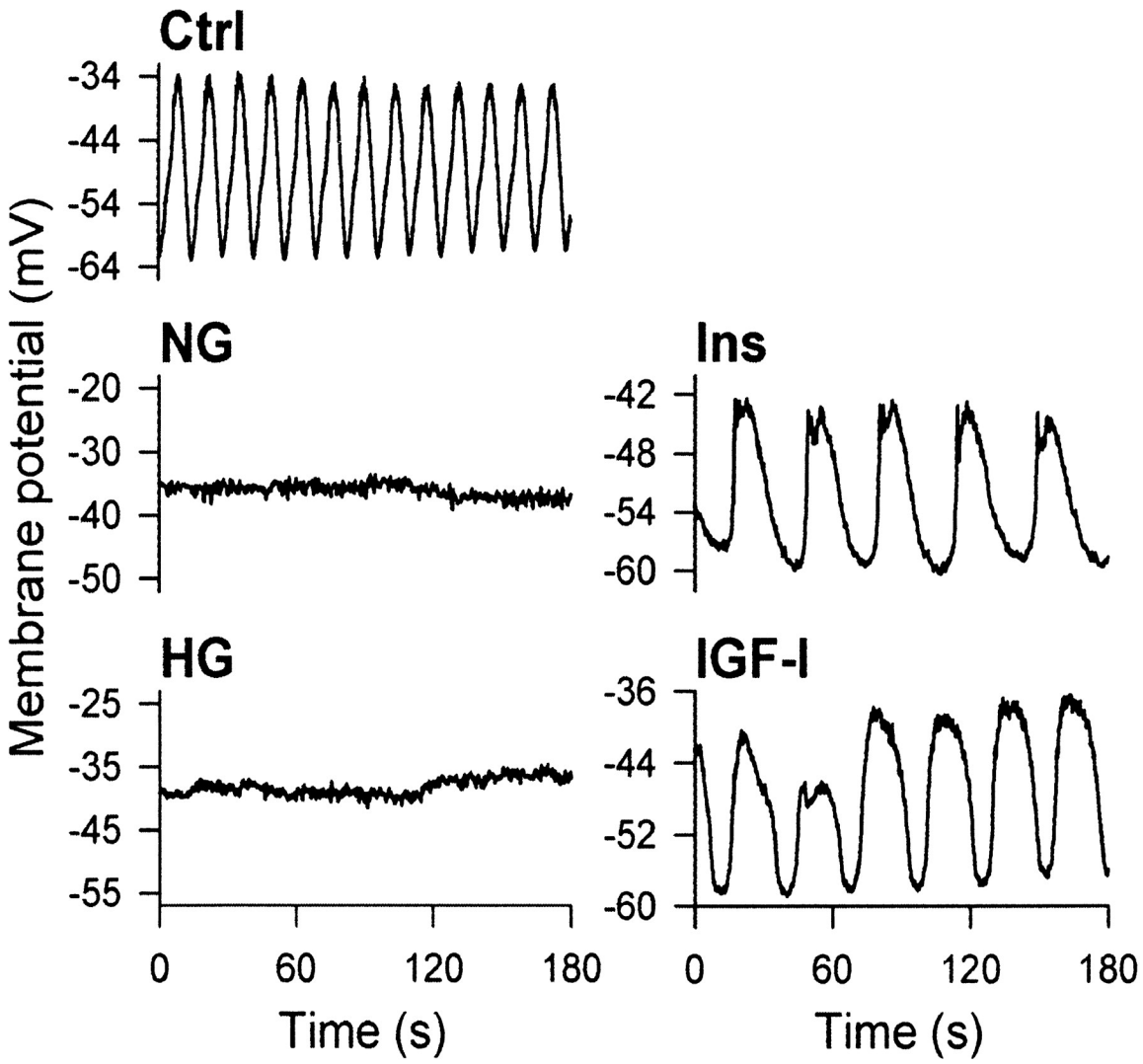

Figure 4. Long-term effects of hyperglycemia, insulin, and IGF-I on gastric slow waves in organotypic cultures. Representative recordings made in freshly dissected controls (Ctrl) and in tissues cultured for 83–86 days in unsupplemented normoglycemic (NG) or hyperglycemic (HG) media or in normoglycemic media containing insulin (Ins) or IGF-I (IGF-I) are shown. Note the lack of slow waves and depolarization of resting membrane potentials in the unsupplemented, normoglycemic, or hyperglycemic cultures. Both depolarization and the loss of slow wave activity were prevented by insulin or IGF-I, although the frequencies in these cultures remained at ~50% of those detected in freshly dissected controls, an effect likely caused by culturing *per se* (57).

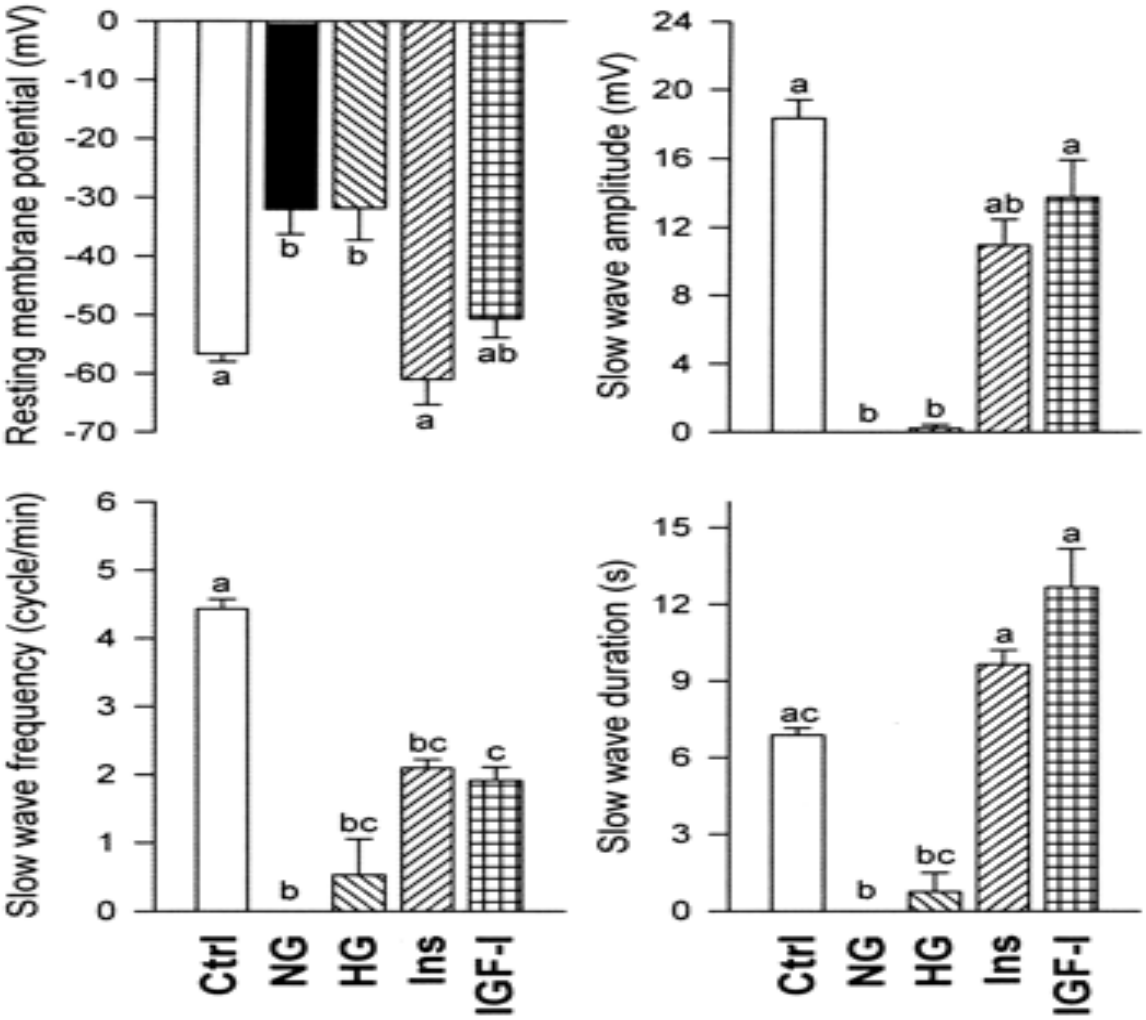

Figure 5. Long-term effects of hyperglycemia, insulin, and IGF-I on gastric slow waves in organotypic cultures. Slow-wave parameters obtained by intracellular impalements (n = 9–16; two tissues per treatment) are shown. Labels correspond to those in Fig. 3. Slow-wave duration was measured at one-half amplitude. ANOVA $P < 0.001$ in all panels; groups not sharing the same superscript are significantly different by multiple comparisons. Slow waves were largely missing in unsupplemented normoglycemic and hyperglycemic cultures. Both insulin and IGF-I prevented the loss of slow-wave activity.

3.3. G*ene expression of FACS purified Cajal cells*

In *in vitro* experiments the depletion of ICC could be completely prevented by the addition of insulin or IGF-1. We were interested in discovering whether ICC express insulin/IGF-1-receptor or not. For this purpose we used ICC populations completely devoid of other cell types present in the gastric *tunica muscularis*. We harvested these cells by using a fluorescence-activated cell sorting technique as described previously (69). We analyzed the expression of messenger RNA (mRNA) for insulin and IGF-I receptors in poor ICC populations and for SCF in ICC populations that were purified from dispersed juvenile (n = 6) or adult (n = 3) BALB/c gastric tunica muscularis tissues by FACS (69). In cell suspensions immunomagnetically depleted of CD11b+ and CD11c+ cells, ICC were identified by FCM as strongly c-Kit+ cells lacking the myeloid markers F4/80 and CD11b and the hematopoietic marker CD45 (Fig. 6*A*). These procedures excluded macrophages and dendritic cells that may take up fluorescent labels nonspecifically and mast cells that also express c-Kit but are strongly CD45 positive (69). The purity of the sorted populations was tested by FCM (Fig 6*B*) and verified by RT-PCR detection of cell-specific markers (Fig 6*C*). Only preparations showing increased c-*kit* expression relative to unsorted cells and lacking mRNA for mast cell chymotryptase (protease 6, *Mcpt6*), smooth-muscle myosin heavy chain 11 (*Myh11*), the neuronal marker protein gene product 9.5 (PGP 9.5; ubiquitin carboxy-terminal hydrolase L1, *Uchl1*), the glial/neuronal marker S100b, the fibroblast/endothelial marker CD34, and the macrophage/dendritic cell marker CD68 (Fig. 6*C*) were analyzed further. Unsorted cells and intact tissue were used as positive controls. ICC populations fulfilling the criteria for purity listed previously (n = 9) did not express mRNA for insulin receptor (*Insr*) or IGF-I receptor (*Igf1r*) (Fig. 6*D*). Likewise, pure ICC also did not express either soluble SCF (*Kitl*[s]) or membrane-bound SCF (*Kitl*[m]), assessed by measuring total (soluble – membrane-bound) SCF mRNA (*Kitl*[s - m]) (72).

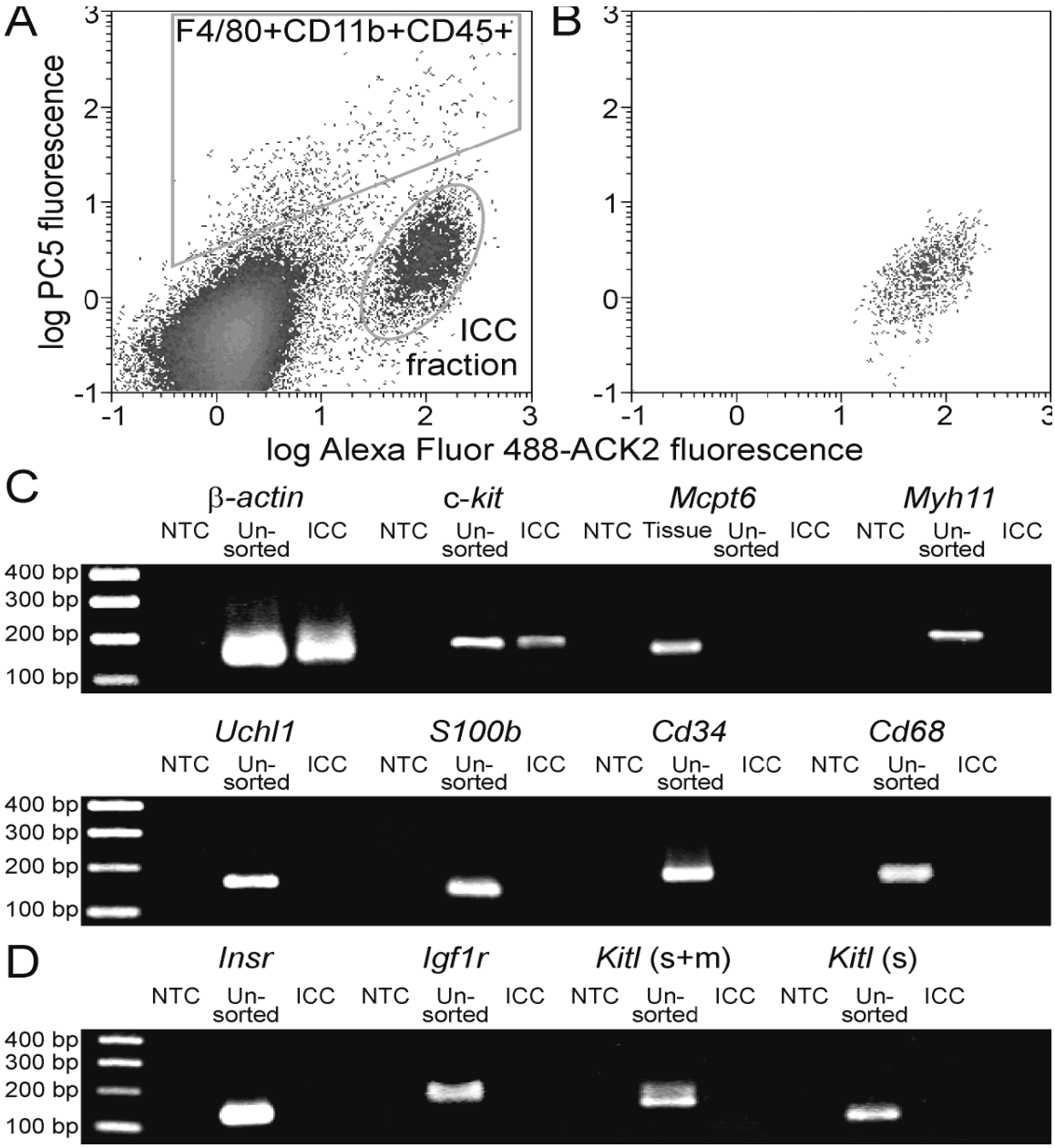

Figure 6. Murine gastric ICC do not express SCF or receptors for insulin or IGF-I. **A**, Gastric ICC were identified by FCM as cells that labeled with anti-c-Kit antibodies (Alexa Fluor 488-ACK2); other potentially c-Kit positive cells were depleted. **B**, Verification by FCM of the purity of ICC populations obtained by FACS. **C**, Verification of the purity of the sorted ICC populations by RT-PCR analysis of the cell-specific mRNA species c-*kit* (ICC, mast cells), *Mcpt6* (mast cells), *Myh11* (smooth muscle), *Uchl1* (neurons), *S100b* (glia, neurons), *Cd34* (fibroblasts, endothelium), and *Cd68* (macrophages, dendritic cells). Unsorted cells and whole tissue were used as positive control. NTC, "no-template" control. Note that sorted ICC only expressed c-*kit* and β-*actin* mRNA. **D**, Lack of *Insr*, *Igf1r* and *Kitl* mRNA in purified ICC. ICC did not express either *Kitl*(s) or *Kitl*(m) as inferred from the absence of *Kitl*(s+m).

3.4. *Localization of insulin-receptor, insulin-like growth factor-I receptor and stem cell factor in gastric tunica muscularis*

Since ICC do not have receptors for insulin and IGF-I, the effects of these growth hormones must be mediated by other cell types having receptors for these growth hormones and possibly producing stem cell factor. Therefore, we next localized insulin and IGF-I receptor and SCF proteins in adult BALB/c (n = 32) and NOD (nondiabetic, n = 5) gastric tunica muscularis tissues. These studies included antibodies to recombinant polypeptides from the insulin receptor α and β subunits, the IGF-I receptor α subunit, and the extracellular portion of SCF (Fig. 7). The results obtained with antibodies to insulin receptor α and β subunits were identical, and, therefore, only results obtained with antibodies to the α subunit are shown. For comparison, Fig. 7*A–D* depict specifically labeled myenteric and intramuscular ICC, myenteric neurons, and intramuscular nerve fibers in the distal stomach. In the gastric corpus and antrum, insulin receptor α immunoreactivity (Fig. 7*E* and *F*) was present throughout both the circular and longitudinal muscle layers. Besides smooth muscle cells, intramuscular fibroblasts may have been stained, too. Strong immunoreactivity was detected in the entire myenteric plexus including ganglion cells (Fig. 7, asterisks), nerve trunks (arrow in Fig. 7*E*) and fine, elongated structures (Fig. 7, arrowheads) that appeared to be intramuscular nerve fibers (Fig. 7*D*) but also resembled intramuscular ICC (Fig. 7*B*). However, double labeling of cryosections with anti–c-Kit antibodies clearly indicated that insulin receptor α- (Fig. 7*F*) and c-Kit-like immunoreactivities (Fig. 7*G*) occurred in closely associated but distinct structures (Fig. 7*H*) and identified the former as nerve fibers that typically accompany intramuscular ICC (70, 71). Anti–IGF-I receptor α antibodies also stained the entire smooth musculature and myenteric plexus (ganglia and nerve trunks) but not intramuscular nerve fibers (Fig. 7*I* and *J*). Similarly to insulin and IGF-I receptors, uniform immunoreactivity for SCF (Fig. 7*K* and *L*) was detected throughout both smooth-muscle layers. Labeled cells may have included intramuscular fibroblasts. However, consistent with earlier reports (77), only the perikarya of a subset of myenteric neurons contained SCF protein.

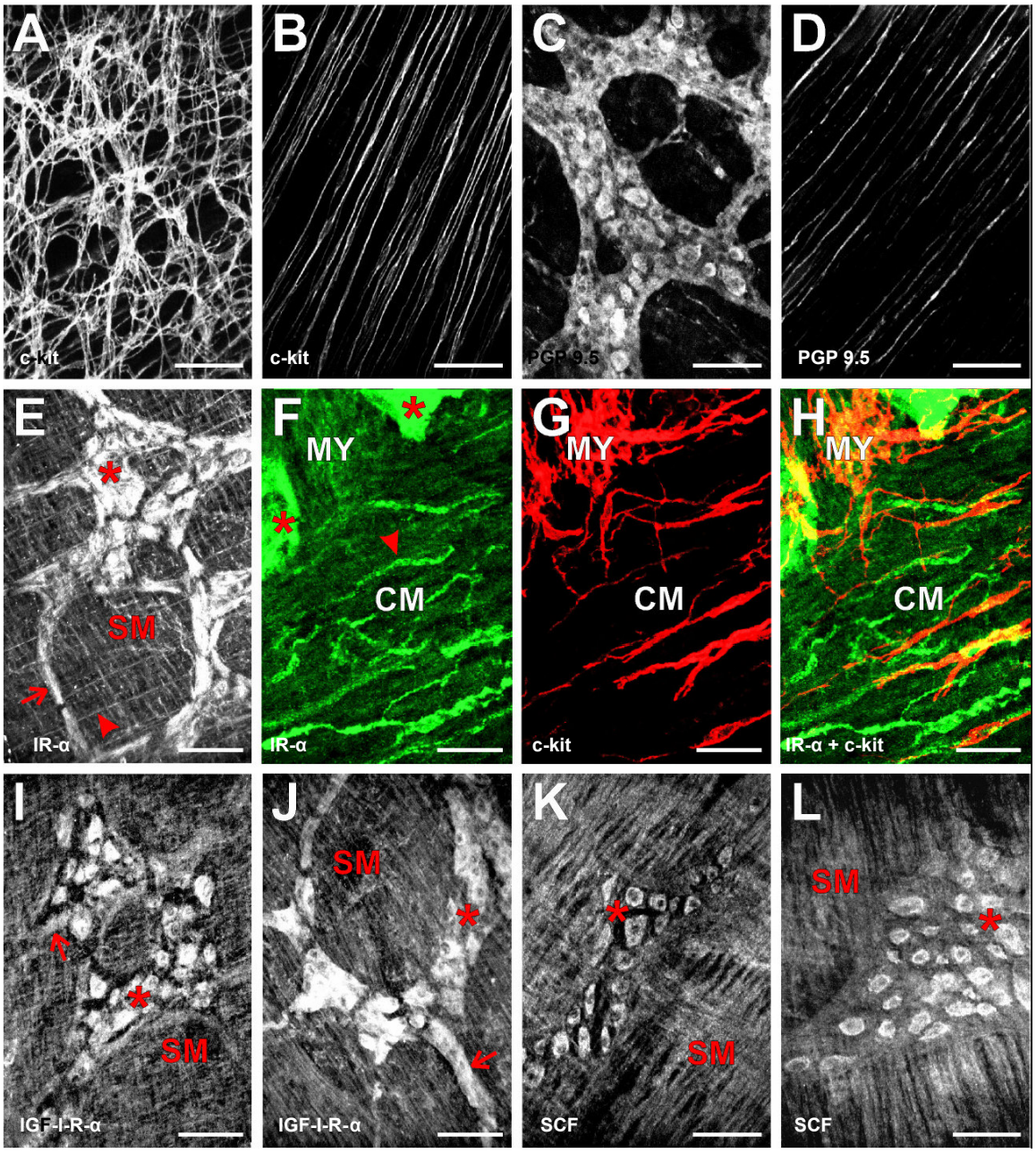

Figure 7. Expression pattern of different markers possibly involved in the diabetes associatied ICC loss of gastric *tunica muscularis*. Scale bars in **F-H** denote 25 μm; in all other panels, 50 μm. It is important to note that cell types which express insulin or IGF-I receptors also have the capability to produce SCF. IR-α: insulin receptor-α. IGF-I receptor-α: IGF-IR-α. See detailed explanation in text (p. 21).

3.5. *Investigation of SCF expression and loss of interstitial cells of Cajal in the stomach of diabetic NOD mice*

The lack of insulin and IGF-I receptors in ICC and their presence in cell types that also express SCF raised the possibility that the effects of these cytokines on ICC could be mediated by SCF. Therefore, we next investigated whether ICC loss in the stomachs of diabetic NOD mice is accompanied by a decline in SCF expression. NOD mice used in this study became diabetic at 182±7 days of age. Gastrointestinal complications developed 56±4 days after the onset of diabetes and, as reported earlier (53) were signified by distended abdominal and gastrointestinal tracts distal to the gastric corpus. The distal colon was always packed with hard feces. Blood glucose levels at the time of sacrifice were above the upper limit of detection (>33.3 mmol/L) in the diabetic mice but were normal in their age-matched littermates used as controls (5.12± 0.19 mmol/L). The depletion of ICC networks was verified by c-Kit immunofluorescence (Fig. 8*A–F*). ICC were clearly reduced in the gastric corpus and antrum of the diabetic animals (Fig. 8*D–F*, $n = 9$) relative to the corresponding regions in their nondiabetic littermates (Fig. 8*A–C*, $n = 11$). Although the myenteric networks were more severely depleted, intramuscular ICC were also affected. The depletion was variable in size and location but always occurred distal to the midcorpus. To examine the role of SCF in these changes, we first extracted data relevant to this problem from genomics databases created by Affymetrix Mouse Genome 430 2.0 GeneChip analysis of gastric corpus+antrum tunica muscularis tissues (fold changes in group means relative to the corresponding control groups are shown in Fig. 8*G*). The depletion of ICC networks in long-term diabetic (60 days) NOD mice (n=3) was reflected by a significant decrease in c-*kit* mRNA expression relative to their nondiabetic littermates (n=3). The decrease in c-*kit* was accompanied by a profound reduction in SCF mRNA, which was detected by 3 different probe sets (*Kitl1-3*). Importantly, the expression of mRNA for smooth-muscle myosin heavy chain (*Myh11*) was also dramatically decreased. In contrast, and consistent with previous reports (6, 7, 11) we found no decline in the expression of the general neuronal marker *Uchl1*. None of these mRNA species changed in short-term diabetes (18 days, n=2 per group; Fig. 8*G*). After 33 days of diabetes (n=2), only *Myh11* was reduced (Fig. 8*G*), thus being the first

marker to decline. The changes in celltype markers were verified by triplicate quantitative RT-PCR analyses of the same samples. SCF and c-*kit* expression was studied in detail by quantitative RT-PCR in a separate set of long-term diabetic (56±4 days, n=8) and nondiabetic mice (n = 9). The results showed that the levels of mRNA for c-*kit* and both the soluble and membrane-bound isoforms of SCF were significantly reduced in the diabetic stomachs (Fig 8*H*). The reduction in smooth muscle myosin and SCF expression in the long-term diabetic animals reflected true atrophy because the dry weight of corpus+antrum tunica muscularis tissues was significantly less in diabetic mice (5.0±0.5 mg, n = 5) than in their nondiabetic, age-matched littermates (7.3±0.5 mg, n = 3, P=0.019).

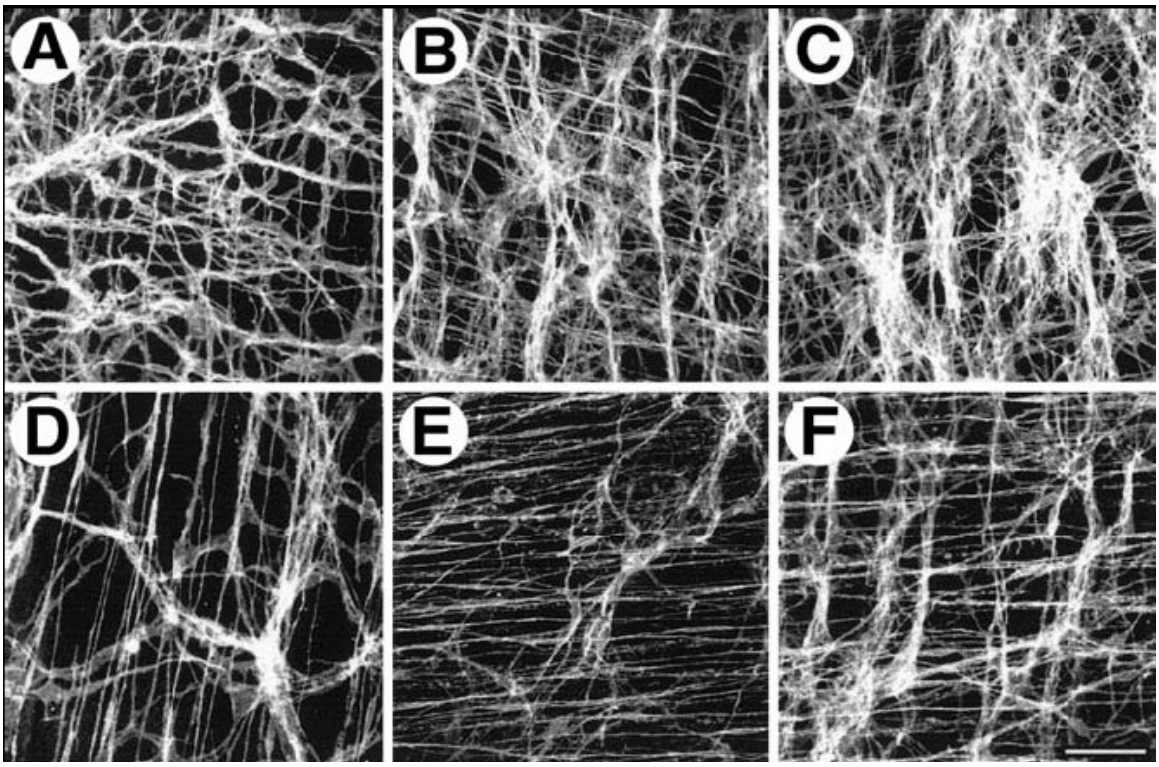

Figure 8 A-F. See explanations on next page.

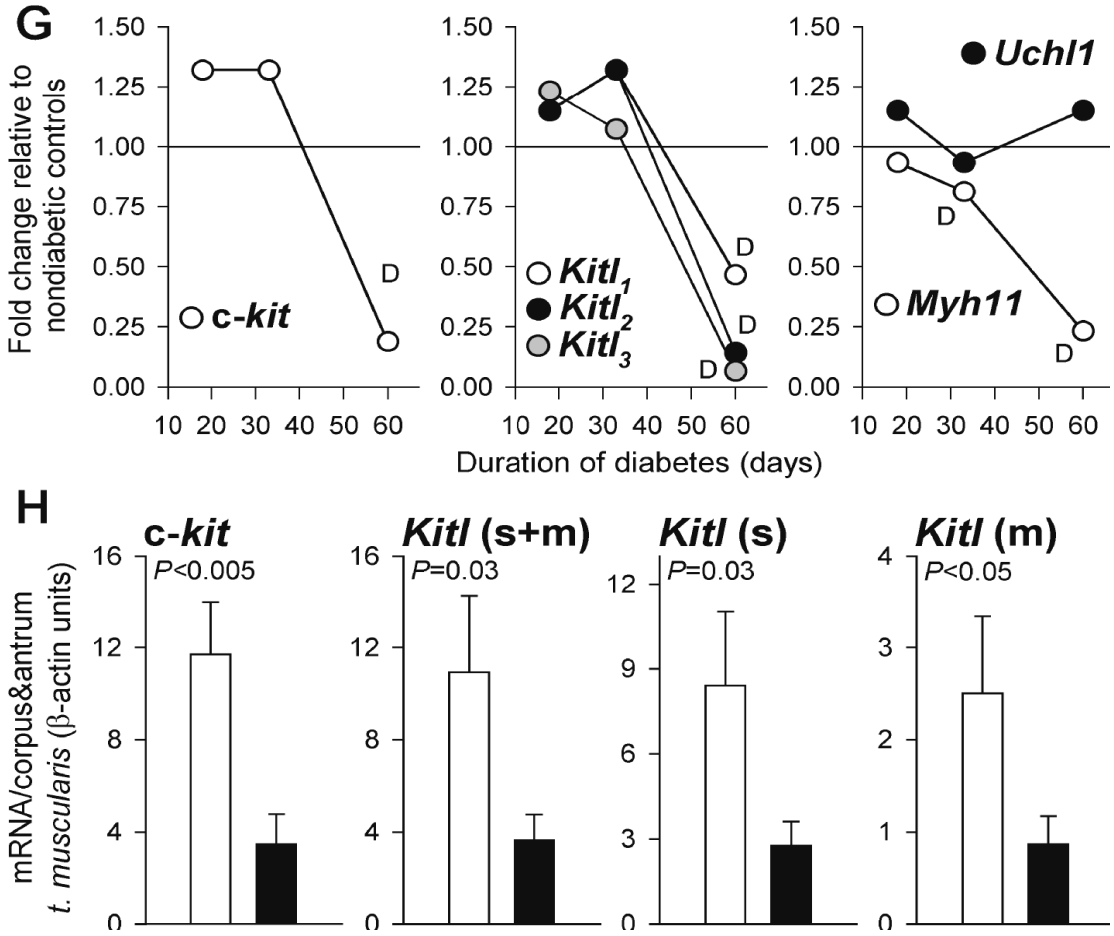

Figure 8. Reduced expression of c-Kit, SCF and smooth muscle myosin in the stomachs of diabetic NOD mice. **A-F**, Representative confocal images of c-Kit immunofluorescence in the greater curvature of full-thickness whole-mounts of gastric *tunica muscularis t*issues of nondiabetic NOD mice (**A-C**) and their long-term diabetic littermates (**D-F**). **A** and **D**, midcorpus; **B** and **E**, orad antrum; **C** and **F**, distal antrum. Scale bar in **F** denotes 50 μm and applies to all panels. Note reduction of c-Kit+ ICC networks in the diabetic mice. **G**, Affymetrix Mouse Genome 430 2.0 GeneChip analysis of c-*kit*, *Kitl*, *Myh11* and *Uchl1* gene expression in NOD mice with short- (18 days), medium- (33 days) and long-term (60 days) diabetes. Fold changes in mean expression levels in groups of diabetic mice relative to groups of their nondiabetic littermates are shown. Values labeled D to be significantly decreased revealed by Affymetrix GeneChip Operating Software analysis (all others: "no change"). Probe sets, statistical definitions, and additional data from the long-term diabetic group are shown in Table 1. **H**, Quantitative RT-PCR analysis of c-*kit* and SCF expression in gastric corpus+antrum *tunica muscularis* tissues of nondiabetic NOD mice (open bars) and their long-term diabetic littermates (closed bars). Expression of *Kitl*(m) was calculated as the difference between *Kitl*(s+m) and *Kitl*(s) in each mouse. *P* values are from Mann−Whitney rank sum tests. Note that the reduction in c-*kit* was mirrored by a similar change in the expression of SCF isoforms.

TABLE

Table 1. Effect of long-term diabetes (60 days) on the expression of selected genes in the gastric corpus+antrum *tunica muscularis* detected by hybridization to Affymetrix Mouse Genome 430 2.0 GeneChip microarrays and analyzed by Affymetrix Gene Chip Operating Software

Description	Affymetrix probe set	NOD nondiabetic			NOD diabetic			NOD diabetic *vs* nondiabetic		
		Signal[A]	Detection[B]	Detection *P*	Signal[A]	Detection[B]	Detection *P*	Signal $\log_2$ ratio	Change[C]	Change *P*
c-*kit*	1415900_a_at	248.6	P	0.001221	38.1	A	0.633789	-2.4	D	0.99998
Kitl$_1$	1415855_at	7449.9	P	0.000244	3199.7	P	0.000244	-1.1	D	0.998923
Kitl$_2$	1426152_a_at	85.7	P	0.023926	16.3	A	0.665527	-2.8	D	0.998799
Kitl$_3$	1448117_at	4062.0	P	0.000244	231.8	A	0.080566	-3.9	D	0.99998
MyHC1	1418122_at	1393.9	P	0.000244	305.1	A	0.095215	-2.1	D	0.999308
Uchl1	1448260_at	2519.5	P	0.000244	3772.0	P	0.000244	0.2	NC	0.757415

A A measure of transcript abundance. The signals in the individual microarrays were background-subtracted, adjusted for noise, and scaled to the same target before comparison.

B Gene expression is called “present” (P) if detection P<0.05 and “absent” (A) if P≥0.065. In each case, all available probe pairs (n=11) were used for making the call.

C The change in the diabetic dataset relative to the nondiabetic dataset is called a “decrease” (D) if change P>(1-0.002) and “no change” (NC) if 0.002667≤P≤(1-0.002667). In each case, intersections of all available probe pairs (n=11) were used.

3.6. *Smooth muscle atrophy and consequent loss of stem cell factor lead to depletion of interstitial cells of Cajal in long term organotypic gastric* tunica muscularis *cultures*

We further investigated the relationship between ICC depletion, loss of SCF and smooth muscle atrophy using long-term organotypic cultures of intact juvenile (14-day-old) BALB/c gastric corpus+antrum muscles (61) (Fig. 9). As it was shown in this study ICC networks and electrical slow waves are maintained in these tissues for 4-6 weeks of culture in unsupplemented normoglycemic media, but deteriorate after 6-10 weeks, by which time ICC, c-*kit* expression, and electrical slow waves are significantly reduced or missing. First we cultured the tissues for 74-75 days in unsupplemented, normoglycemic (5.55 mmol/l) basal media (Fig. 9, NG), or in basal media supplemented with either high glucose (55.5 mmol/l; HG) or 5 μg/ml insulin (Ins) or 100 ng/ml IGF-I. The effects of these treatments on SCF isoforms (n = 5/group) and markers specific for ICC, smooth muscle cells and neurons (n = 7/group) were analyzed by quantitative RT-PCR. The effects on c-*kit* expression were similar to our previous findings. Relative to freshly dissected control tissues (Fig. 9, Ctrl), c-*kit* was dramatically reduced in cultures maintained with unsupplemented, normoglycemic or hyperglycemic media, and this decrease was significantly prevented by insulin and IGF-I supplementation. By immunohistochemistry we have demonstrated in this study that these changes in c-*kit* expression are paralleled by corresponding changes in ICC network densities. Significant contribution of mast cells to c-*kit* mRNA in these studies is also unlikely because normal murine gastric *tunica muscularis* tissues devoid of mucosal or submucosal contamination only contain negligible amounts of *Mcpt6* transcripts (note lack of *Mcpt6* expression in unsorted *tunica muscularis* cells in Fig. 6C and see Ref 72). The changes in c-*kit* were mirrored by similar trends in SCF (*Kitl*) expression except that IGF-I stimulated the membrane-bound isoform well beyond control levels, whereas changes in *Kitl*(s) did not reach statistical significance. The effects of the treatments on the expression of the smooth muscle-specific gene *Myh11* were similar to the changes in c-*kit* and *Kitl*. In contrast, mRNA for the neuronal marker *Uchl1* was undetectable in most cultures regardless of media supplementation (Fig. 9).

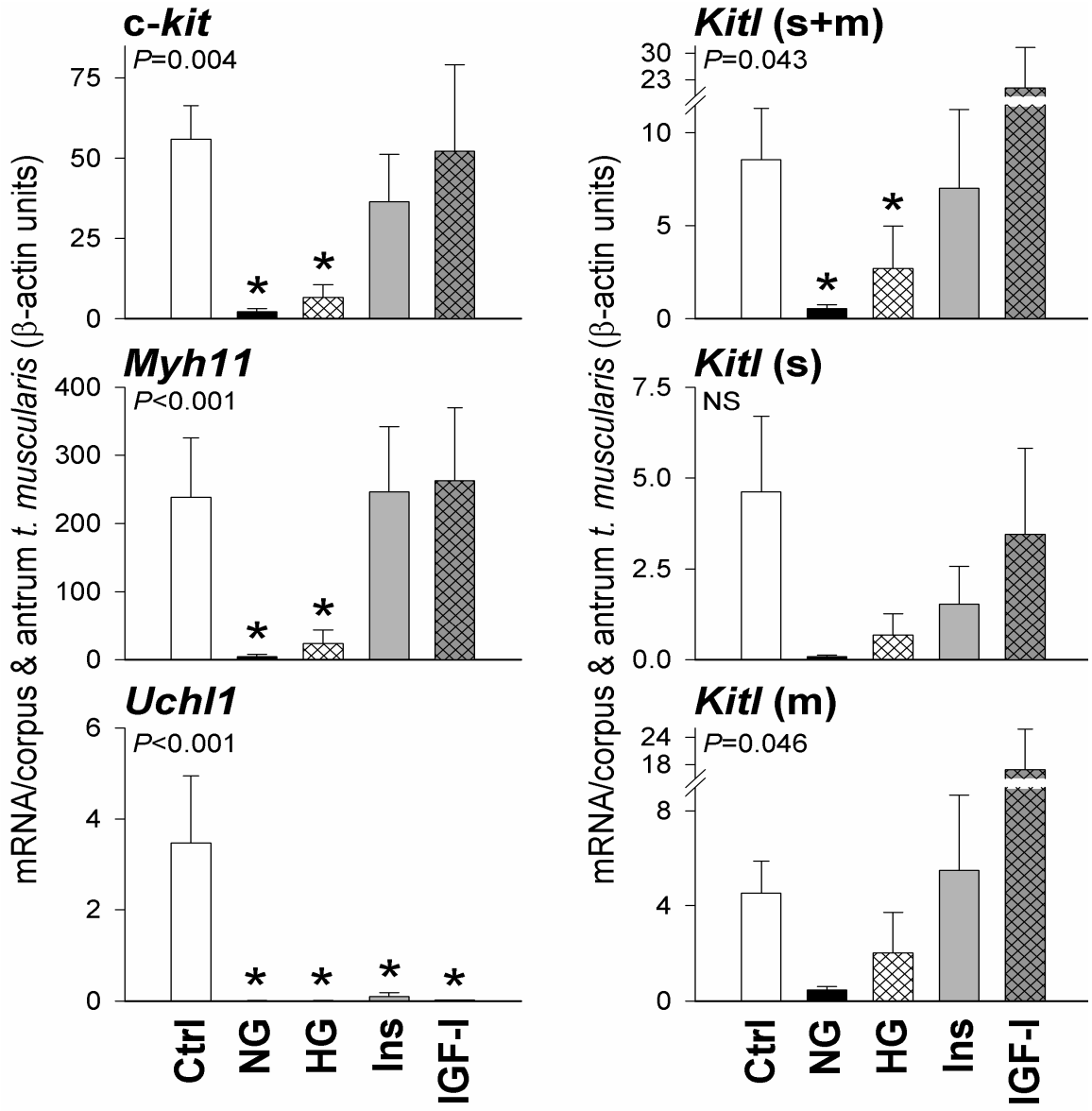

Figure 9. Role of SCF produced by smooth muscle cells in the long-term maintenance of ICC: Long-term effects of growth factor deprivation (in the presence of normo- or hyperglycemia) and insulin or IGF-I supplementation on the expression of c-*kit*, *Myh11*, *Uchl1* and SCF (*Kitl*) isoforms (*soluble* (s); *membrane bound* (m)) measured by quantitative RT-PCR. Ctrl: freshly dissected control gastric *tunica muscularis* tissues. The other groups are tissues cultured for 74-75 days with either unsupplemented, normoglycemic media (NG), hyperglycemic media (HG), normoglycemic media containing insulin (Ins), or normoglycemic media supplemented with IGF-I (IGF-I). *P* values are from Kruskal–Wallis one-way ANOVA on ranks; groups labeled with asterisks are significantly different from Ctrl by Dunn's *post-hoc* multiple comparisons. The decrease in c-*kit* expression in the long-term normo- and hyperglycemic cultures and the prevention of this change by insulin or IGF-I were paralleled by similar changes in *Myh11* and SCF isoforms. *Uchl1* expression was lost in all cultures regardless of treatment.

3.7. *Relationship between ICC loss and stem cell factor producing cells*

The data presented in Fig. 8*G* and 9 clearly indicate that smooth-muscle cells and myenteric neurons, the two main sources of SCF in the gut (72-74) differ in their relationship to ICC; whereas changes in the smooth muscle always mirrored the changes in ICC and *Kitl* expression, neuronspecific gene expression remained normal in long-term diabetic NOD mice with depleted ICC (Fig. 8*G*) and stayed near undetectable levels in the insulin- and IGF-I–treated organotypic cultures despite the rescue of the ICC networks (Fig. 9). We investigated whether intracellular localization of SCF in myenteric neurons (74) could account for the dramatic dissociation between the fates of neurons and ICC. As shown in Figure 10, live immunolabeling of tunica muscularis tissues from BALB/c and nondiabetic NOD mice (n = 7) only stained the membranes of circular and longitudinal smooth-muscle cells, and no surface labeling of myenteric ganglion cells was detectable. Thus, SCF produced by myenteric neurons may not be available for the ICC.

3.8. *Immunoneutralization of stem cell factor accelerate the loss of gastric ICC*

Because we had previously demonstrated that the blockade of c-Kit signaling with ACK2 anti–c-Kit antibody accelerated the demise of gastric ICC networks in organotypic cultures (57) we examined whether these results could be replicated by immunoneutralization of SCF, the natural ligand for c-Kit (Fig. 11). As revealed earlier, (57) culturing corpus+antrum muscles from juvenile BALB/c mice in unsupplemented, normoglycemic basal media for 34 days did not affect ICC network morphology (Fig. 11*A*), although c-*kit* mRNA levels in these cultured control tissues (open bar in Fig. 11*C*, n = 3) were already lower than in freshly dissected tissues (open bar in Fig. 9, c-*kit* panel). Inclusion of polyclonal anti-SCF antibodies (2 μg/ml) in the culture media caused a profound depletion of both main ICC classes (Fig. 11*B*) and a significant reduction of c-*kit* expression (Fig. 11*C*, n = 3), indicating that loss of SCF *per se* can lead to loss of ICC.

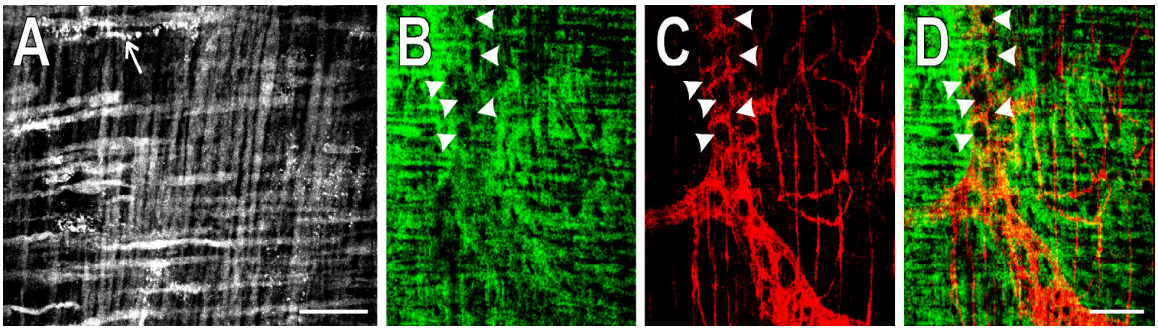

Figure 10. Myenteric neurons, unlike smooth muscle cells, do not express SCF protein on their surface. Live *tunica muscularis* tissues were incubated with anti-SCF antibodies at 4 °C for 3 h before fixation with 4% paraformaldehyde-saline. SCF-like immunoreactivity in the whole mounts was visualized with Alexa Fluor 488-conjugated secondary antibodies (panel **A** and green color in panels **B** and **D**). In the experiment illustrated in **B-D**, neural fibers were counterstained with monoclonal antibodies against neural cell adhesion molecule (CD56) before fixation and developed with Alexa Fluor 594-labeled secondary antibodies (red color in **C** and **D**). **D**: composite of **B** and **C**. In Panel **A** presents a confocal projection of 2 optical sections representing the perimyenteric region is shown. Note that no SCF-immunoreactive myenteric neurons appear between the circular (vertical) and longitudinal muscle layers. Arrow points at punctate staining in a macrophage that phagocytosed the primary antibody. Panels **B-D** show a single optical section taken with an enlarged confocal aperture to allow simultaneous visualization of a myenteric ganglion (**C**) in the focal plane and SCF on the surface of muscle fibers in the circular and longitudinal layers immediately above and below the focal plane (**B**). The anti-CD56 antibody only labeled neural fibers and left the perikarya of myenteric neurons unstained (arrowheads in **C**). Many of the same areas also remained unstained in the green fluorescent channel (arrowheads in **B** and **D**), whereas others only contained projected SCF-like immunofluorescence from muscle fibers displaced by the neural structures. The circular muscle fibers outlining the ganglion should also be noted. No evidence of cell surface-expression of SCF by myenteric neurons was found (compare panels **A** and **B** with Fig. 7 K and L). Scale bars denote 50 μm.

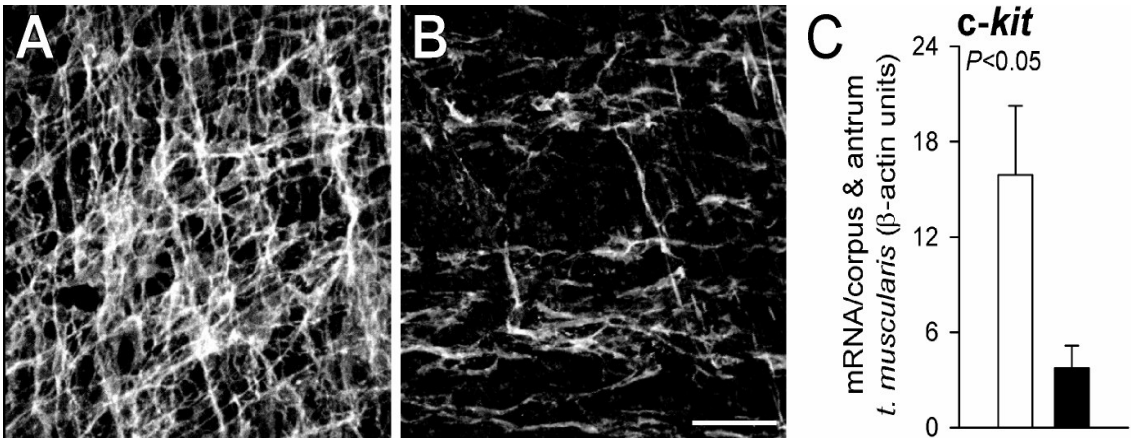

Figure 11. Role of SCF produced by smooth muscle cells in the long-term maintenance of ICC: Effects of polyclonal antibodies against the extracellular/soluble portion of SCF on ICC networks and c-*kit* expression. **A** and **B**: representative confocal images of c-Kit-like immunofluorescence in juvenile murine gastric corpus+antrum *tunica muscularis* tissues cultured for 34 days with unsupplemented, normoglycemic media in the absence (**A**) or presence (**B**) of 2 μg/ml anti-SCF antibodies. Scale bar in **B** denotes 50 μm and applies to both panels. **C**, Effects of immunoneutralization of SCF on c-*kit* expression measured by quantitative RT-PCR. Open bar: controls; closed bar: anti-SCF-treated. The *P* value is from unpaired Student *t*-test. Note profound reduction of ICC and c-*kit* expression by the anti-SCF antibody.

Discussion

The main objectives of this study comprised first, to establish long-term organotypic cultures of murine gastrointestinal tract tissue to clarify the role of hyperglycaemia, insulin and IGF-I in the impairment of ICC morphology and function induced by diabetes mellitus and, second, by using this technique together with other methods to explore the mechanisms responsible for this ICC damage.

4.1. *Role of hyperglycaemia, insulin and IGF-I in the maintenance of Cajal cell morphology and function*

In the first part of our study we used organotypic cultures of gastric corpus and antrum tunica muscularis to dissect the contributions of hyperglycemia and insulinopenia to diabetes-associated ICC loss (25, 26, 53-55). Our results demonstrated that normal ICC network morphology is completely unaffected by long-term hyperglycemia. This observation was surprising since chronic complications of diabetes are generally attributed to recurring episodes of hyperglycemia and resultant oxidative damage, nonenzymatic glycation, and activation of protein kinase C, nuclear factor {kappa}B and aldose reductase (59). Hyperglycemia has been shown to induce apoptosis via activation of caspase-3 in cultured superior cervical ganglia, dorsal root ganglion neurons, Schwann cells and neuroblastoma cells, and only a relatively small proportion of these effects can be attributed to hyperosmolarity (58, 75). It is unclear why ICC are not damaged by hyperglycemia, but it is noteworthy that they contain an abundance of mitochondria and rely on oxidative metabolism for electrical pacemaking (32) and thus probably possess efficient mechanisms for elimination of superoxide and other reactive oxygen species (61). Even more surprising was the finding that hyperglycemia can actually limit the damage to ICC networks that occurs between 34 and 68 days of culture. High levels of glucose (up to 100 mmol/l) have been reported to have paradoxical neuroprotective effects against glutamate and free radical neurotoxicity and oxygen-glucose deprivation by enhancing mitochondrial transmembrane potentials (76). Glucose can also activate members of the mitogen-activated protein kinase family (77) and may stimulate the production of tissue growth factors required for ICC survival and function. Whether any of these mechanisms contribute to the observed effects remains to be investigated. It is also important to note that hyperglycemia could not prevent the loss of electrical slow waves, suggesting an inhibition of pacemaking independent of ICC depletion. This observation is consistent with previous findings that even acute elevations in blood glucose levels can have deleterious effects on gastrointestinal motility by eliciting gastric dysrhythmias, impaired antroduodenal motor activity, delayed gastric emptying, altered visceral sensation, and impaired colonic response to feeding (45-47, 58). It is therefore

likely that acute hyperglycemic episodes in diabetes may interact with ICC loss precipitated by other mechanisms to cause acute exacerbations of chronic symptoms in various manifestations of diabetic gastroenteropathies (45, 58).

When gastric or small intestinal muscles are isolated from newborn mice and cultured in normoglycemic unsupplemented basal media, ICC and electrical slow waves continue to develop for at least 10 days (78) and are maintained for about a month. These findings indicate that the tunica muscularis has intrinsic reserves from which ICC can draw for normal function. However, ICC networks begin to deteriorate around 6 weeks (57) and, as we have demonstrate here, undergo significant depletion by the end of the 10th week of culture, following a time course similar to the ICC loss that occurs in untreated diabetic NOD/LtJ mice (53). The decline in ICC is paralleled by a similar disruption of electrical slow waves (53, 57). These changes can be accelerated by continuous blockade of c-Kit signaling with the neutralizing antibody ACK2, indicating that stem cell factor, the natural ligand for c-Kit, plays a critical role in the maintenance of the ICC phenotype not only *in vivo* (16, 18), but also in culture (57, 78), and that endogenous production of this cytokine may require additional (likely serum-born) factors beyond a certain period of time. This dependence on extrinsic factors is more evident in canine (79) and mouse colon tissues placed in culture (T.Ö., unpublished data), where ICC and smooth muscle cells require serum supplementation for survival. In this study, we demonstrate that insulin is an important serum-born factor required for the long-term maintenance of ICC. The depletion of ICC networks could be completely prevented by insulin treatment, even in the presence of 55.5 mmol/l glucose, and these effects were not enhanced any further by the administration of 5% fetal bovine serum. In fact, we have shown that c-Kit–like immunoreactivity, c-kit expression, and electrical slow-wave activity in ICC can be maintained for at least 86 days under these circumstances, except for an ~50% reduction in slow-wave frequency, which is likely to be an effect of culturing *per se* (57). Recently, we have found that insulin treatment can also prevent ICC loss in gastric antrum tissues obtained from adult BALB/c mice (unpublished data). These results strongly suggest that insulinopenia may be the underlying cause of ICC loss and resultant deterioration of electrical pacemaking and gastroparesis in diabetic NOD/LtJ mice (53) and, possibly, in patients with diabetes (25, 26, 55, 58). Although chronic complications of diabetes have

been traditionally attributed to hyperglycemia (59), it is now well established that reduced or ineffective insulin signaling and abnormal levels of other growth factors also play important roles (61), even in type 2 diabetes, where blunted glucose-induced insulin secretion accompanies insulin resistance in target tissues (60). The lower prevalence of gastropathy in type 2 diabetes (up to 30% vs. 50% in type 1 diabetes) (46) also supports a role for absolute or relative insulinopenia in this complication. Furthermore, 1-week insulin treatment has been reported to restore delayed liquid emptying in NOD mice by stimulating neuronal nitric oxide synthase expression, an effect that could not be replicated by acute normalization of blood glucose levels (62). Thus, insulin may have multiple beneficial effects on diabetes-associated gastric motor dysfunction.

The disruption of ICC networks in our studies could also be prevented by IGF-I supplementation. Circulating IGF-I levels do not appear to correlate with the degree of glycemic control and are reduced in both type 1 and type 2 diabetes, although the changes are less pronounced in the latter (61). IGF-I may mediate, at least in part, the effects of insulin, which is known to stimulate IGF-I expression (61). Since insulin and IGF-I and their receptors are structurally related, cross-talk between the two systems may also occur at pharmacological concentrations (61, 80). Insulin may also be able to activate signaling through the IGF-I receptor ß subunit at physiological concentrations by binding to hybrid insulin/IGF-I receptors containing the A isoform of insulin receptor (80). However, it is unclear whether such hybrid receptors can be found in the gastrointestinal tunica muscularis. In any case, the finding that both insulin and IGF-I can prevent the loss of ICC suggests that these effects are more likely to be mediated by genomic, rather than metabolic, actions of insulin (61). The intracellular pathways involved in the long-term maintenance of the ICC phenotype by insulin and IGF-I remain to be investigated.

It is important to emphasize that in addition to insulin and IGF-I, other factors may also contribute to the long-term maintenance of ICC and electrical slow waves. For example, IGF-II, another natural ligand for the IGF-I receptor, may have effects similar to IGF-I (rev. in 61). In addition, the proinsulin C-peptide has been shown to enhance or mimic the effects of insulin and to normalize the expression of insulin receptor, IGF-I, and IGF-I

receptor in peripheral nerves of diabetic rats (rev. in 61). Elucidation of the role of these factors on ICC requires further investigation.

Results we got from the long term tissue cultures indicate that the diabetes-associated depletion of ICC, a significant component of diabetic gastropathy and gastroparesis, is unlikely to be caused by chronic or recurrent hyperglycemia. In contrast, maintenance of ICC requires insulin or IGF-I, which are reduced or ineffective in diabetes.

4.2. *Role of insulin and IGF-I in the maintenance of Cajal cell morphology and its impairment by diabetes mellitus*

Since ICC damage in long term diabetes is likely to be a consequence of reduced insulin and/or IGF-I signaling, in the second part of the study we first examined whether ICC is a direct target of the abovementioned growth factors. Our data obtained by using FACS, qualitative PCR and immunohistochemistry clearly indicate that mature ICC do not express receptors for insulin and IGF-I. We found insulin receptor α and β and IGF-I receptor α immunoreactivity only in the smooth muscle layers, myenteric neurons and, in the case of insulin receptor α, intramuscular nerve fibers. Consequent with these data we could not detect transcripts for insulin and IGF-I receptor in ICC populations purified by FACS. The same cell types that had insulin and IGF-I receptors were also found to express SCF, which is required for long-term ICC survival and function (38, 57, 70-74). Therefore, we examined whether SCF could mediate the dramatic protective effect of insulin and IGF-I on slow waves and ICC and whether a decline in SCF production could be responsible, at least in part, for the ICC depletion of diabetes. We used several approaches to prove this protective role of SCF. By using quantitative PCR and RNA hybridization methods we have shown that in the stomach of long-term NOD diabetic mice reduction of ICC and c-Kit expression was mirrored by a similar decline of the expression of both soluble and membrane bound stem cell factor. By using long-term organotypic gastric *tunica muscularis* cultures we also showed that insulin and IGF-I supplementation have a similar effect on c-Kit and SCF (both soluble and membrane

bound) expression: the two markers changed parallel. To further reinforce these data we used immunoneutralization of SCF in organotypic cultures. Using this technique we have shown that application of anti-c-*kit* antibody led to a loss of both main ICC classes closely resembling the depletion elicited by insulin/IGF-I deficiency. The latter finding complements our earlier results that established the dependence of gastric ICC on c-Kit signaling (57). In those studies, we found that chronic anti-c-Kit antibody blockade of SCF signaling through c-Kit receptors caused the disruption and eventual loss of both myenteric and intramuscular ICC networks, leading to loss of electrical slow waves and responses to electrical stimulation. The anti-c-Kit treatment was specific for ICC because the smooth musculature continued to respond normally to acetylcholine or elevated external K+ concentration (57). The role of SCF/c-Kit signaling in the maintenance of gastric ICC is also supported by the near-complete loss of intramuscular ICC (70) and the significant, quantitative reduction of myenteric ICC (56, 81) in the stomachs of *W/WV* mice that have reduced (but not lost) c-Kit tyrosine kinase activity (82). Clearly, these previous and the present results provide strong support for the notion that most gastric ICC depend on uninterrupted SCF signaling through c-Kit. It follows that the demonstrated reduction in SCF production in the diabetic stomachs must also play a significant role in the decrease in ICC network densities that occurs in this disease. However, studies in *W/WV* and *Sl/Sld* mice suggest that the degree of SCF requirement of ICC depends on both the ICC class (myenteric ICC are better preserved than intramuscular ICC) and anatomic localization (myenteric ICC are nearly normal in the greater curvature of the distal antrum, whereas they are profoundly reduced elsewhere in the stomach) (56, 71, 79). Thus, SCF, however important, may not be the primary survival signal for some ICC, which may require other factors for maintenance and function. The extent to which these other, putative factors contribute to the pathogenesis of diabetic gastroparesis remains to be investigated.

Although the data we presented here theoretically could be a basis of a therapeutic use of stem cell factor in diabetic gastroparesis, there may be some possible disadvantages of the therapeutic use of this cytokine. As it has been clearly demonstrated, the decrease of SCF expression in diabetes is likely to result from a reduction in the number of cells that normally present this signal to ICC, i.e. smooth-muscle atrophy, rather than a reduced

stimulation of *Kitl* transcription by insulin and/or IGF-I. Therefore, administration of SCF could not improve the major pathological impairment, i.e. smooth muscle atrophy which appears to be the ultimate cause of ICC depletion. Moreover, effective support of ICC would require the delivery of membrane-bound SCF, the isoform that can provide biologically significant stimulation of c-Kit signaling (83) to ICC (*e.g.* by targeted overexpression in gastric smooth-muscle cells). However, because signaling by membrane-bound SCF is spatially restricted, even the higher-than-normal levels in the surviving smooth-muscle cells would not be able to compensate for the loss of SCF that occurs in the atrophied regions. In contrast, because SCF expression faithfully follows the changes in smooth-muscle–specific gene expression both in vitro and in vivo, treatments that could reverse or preserve smooth-muscle mass should not only prevent or correct myopathy but also efficiently raise or maintain SCF levels and protect ICC. There have been several previous attempts to identify the sources of SCF for ICC development and maintenance (72-74, 84). Early studies in SCF-lacZ transgenic mice could only identify myenteric neurons as potential sources of SCF (72). However, a role for smooth muscle cells was strongly suggested by findings of normal ICC in the absence of an enteric nervous system (73, 84) and non-neuronal cells expressing SCF protein were later identified by immunohistochemistry (74). Epperson *et al* (85) also detected SCF mRNA in smooth muscle cells and in single ICC in cell suspensions prepared from fundic and small intestinal muscles and sucked into micropipettes. In this study, we localized SCF protein in myenteric neurons and smooth-muscle cells throughout the gastrointestinal tract by immunohistochemistry and failed to detect either SCF protein or mRNA in gastric ICC. It is important to note that since the latter results were obtained in populations of 20,000 –100,000 ICC purified by FACS and rigorously tested for purity by FCM and RT-PCR in each experiment, they provide strong evidence that ICC do not contribute to their own maintenance.

Our data obtained by RNA hybridization also confirm that myenteric neurons, unlike smooth-muscle cells, are probably not decreased in diabetic gastroparesis, (62, 86, 87) although reduced density of intramuscular nerve fibers has been reported in a case of advanced diabetic pseudo-obstruction (25). However, reduced production of neuron-derived factors could also manifest at the functional or gene expression level (45, 62, 86).

Indeed, short-term insulin treatment has been reported to correct reduced neuronal nitric oxide synthase expression in mice (62). However, in our studies, both IGF-I and insulin were able to rescue gastric ICC and smooth-muscle cells without preventing the complete loss of neurons in unsupplemented organotypic cultures. Thus, even if ICC depended on some neuron-derived factors and even if those factors were reduced in diabetes, insulin and IGF-I treatments must be able to compensate fully for their missing effects even in the absence of neurons. In summary, these results clearly indicate that the fate of ICC in diabetes depends on SCF from smooth-muscle cells but probably not from myenteric neurons. A similar conclusion has been reached in studies on the development of ICC (73, 74, 84). A predominantly intracellular localization of SCF in myenteric neurons could account for the lack of neuronal effects on ICC maintenance (74). Because both the "soluble" and "membrane-bound" isoforms of SCF exist as extracellular portions of a transmembrane protein, (24, 83, 85) these observations suggest that SCF in myenteric neurons may lack a membrane localization signal (24). As discussed earlier, our data strongly indicate that insulin and IGF-I probably increase SCF levels, at least in part, by preventing smooth-muscle atrophy (87-89) Pathways whereby IGF-I stimulates smooth muscle cell growth have been described and include activation of phosphatidyl inositol-3-kinase, 3-phosphinositide–dependent kinase-1 and the 70-kDa ribosomal S6 kinase (90). IGF-I can also prevent apoptosis in these cells by inhibiting glycogen synthase kinase-3β (91). Insulin also has antiapoptotic effects (35). Insulin and IGF-I–signaling mechanisms overlap considerably and cross-talk between them can occur at both physiological and pharmacological levels (80). In our studies, IGF-I typically had greater effects on gene expression than insulin, despite being used at a lower concentration. Therefore, it is likely that the observed effects were primarily mediated by IGF-I receptors. In addition to preserving SCF levels by preventing the loss of their main source, insulin and IGF-I may directly stimulate SCF expression (*e.g.* via the mitogen activated protein kinase cascade) (90, 93). However, the existence of transcriptional control of SCF by these cytokines is uncertain and remains to be investigated. An SCF-mediated link between smooth muscle and ICC may also underlie ICC loss in other diseases (*e.g.* the myopathic forms of intestinal pseudo-obstruction, where both cell types undergo atrophy) (22). However, ICC loss is also known to accompany conditions in which smooth-muscle mass is not

reduced (94) or where it is increased (*e.g.* in partial mechanical obstruction) (95). The disparate behavior of ICC and smooth muscle cells in these cases might result from a decrease in SCF without smooth-muscle atrophy or the existence of mechanisms for ICC loss that are independent of SCF/c-Kit signaling, such as leukocytic infiltration or altered cytokine and nitric oxide secretion, which may also contribute to the diabetes-associated ICC depletion (96). It follows from the foregoing that myopathy precipitated by reduced insulin/IGF-I signaling may play a more central role in gastrointestinal complications of diabetes than previously recognized. Smooth muscle atrophy (87-89) besides causing weakness and hypomotility of antral muscles, may lead to all the well-established consequences of ICC loss including electrical dysrhythmias (56, 57), reduced peristalsis and delayed solid emptying (53-55), impaired neural control via ineffective excitatory and inhibitory neuromuscular neurotransmission (70, 71) and vagally mediated mechanoreception (38). Because manifestations of these changes have been shown in both patients and animal models with diabetic gastropathy and gastroparesis (45, 53-55, 63, 97) many of the most important gastrointestinal dysfunctions in diabetes may be the indirect consequence of myopathy. Furthermore, when gastroparesis occurs in the absence of systemic autonomic neuropathy demonstrable by clinical tests (97-99), ICC defects caused by loss of SCF from the smooth muscle may mimic some of the signs and symptoms of neuropathy such as altered visceral sensitivity, impaired receptive and sphincter relaxation, electrical dysrhythmias, and delayed emptying (38, 53, 56, 57, 70, 71) by disrupting communication between sensory and motor nerves and the smooth musculature. Myopathy, a somewhat overlooked aspect of diabetic gastroenteropathies, may have consequences far beyond reduced contractility by causing the depletions of ICC networks. In turn, pharmacological perturbation of smooth muscle function may represent an important target for the prevention and treatment of diabetic gastroparesis.

In conclusion, the present study has revealed new aspects of the pathophysiology and of diabetes-induced motility disorders of the gastrointestinal tract. In contrast with recent views, the present findings furnished evidence for smooth muscle dysfunction as a primary pathological cause of diabetic gastroparesis. Impairment of Cajal cell function and consequent changes in gastric motility appear to result from smooth muscle atrophy

rather than from disrupted cytokine signaling or neuronal function. Moreover, the findings may offer new possibilities in the management of motility disorders of the gastrointestinal tract.

References

1, **Cajal SR.** Sur les ganglions et plexus nerveux de l'intestin. *CR Soc Biol (Paris)*; 45: 217-223, 1893

2, **Cajal SR.** Histologie du systeÁme nerveux de l'homme et des verteÂbreÂs, 2. Paris: Maloine, 891-942, 1911

3, **Taxi J.** Contribution aÂ l'eÂtude des connexions des neurons moteurs du systeme nerveux sutonome. *Ann Sci Nat Zool Biol Anim* 7: 413-674, 1965

4, **Duchon G, Henderson R, Daniel EE.** Circular muscle layers in the small intestine. *In: Daniel EE, ed. Proc 4th Int Symposium Gastrointestinal Motility.* Vancouver, Canada: Mitchell, 635-46, 1974.

5, **Imaizumi M, Hama K.** An electromicroscopic study on the interstitial cells of the gizzard in the love bird (Uronloncha domestica). *Z Zellforsch Mikrosk Anat* 97: 351-7, 1969

6, **Cook RD, Burnstock G.** The ultrastructure of Auerbach's plexus in the guinea-pig. II Non-neuronal elements. *J Neurocytol* 5: 195±206, 1976

7, **Gabella G.** Fine structure of the myenteric plexus in the guinea-pig ileum. *J Anat* 111: 69-97, 1972

8, **Komuro T.** Three-dimensional observation of the fibroblast-like cells associated with the rat myenteric plexus, with special reference to the interstitial cells of Cajal. *Cell Tiss Res* 255: 343-51, 1989

9, **Richardson KC.** Electron microscopic observations on Auerbach's plexus in the rabbit, with special reference to the problem of smooth muscle innervation. *An J Anat* 103: 99-136, 1958

10, **Rogers DC, Burnstock G.** The interstitial cell and its place in the concept of the autonomic ground plexus. *J Comp Neurol* 126: 255-84, 1966

11, **Thuneberg L.** Interstitial cells of Cajal: intestinal pacemaker cells. *Adv Anat Embry Cell Biol* 71: 1-130, 1982

12, **Faussone-Pellegrini MS, Cortesini C, Romagnoli P.** Sull'ultrastruttura della tunica muscolare della prozione cardiale dell'esofago e dello stomaco umano con particolare

riferimento alle cosiddette cellule inerstiziali di Cajal. *Arch Ital Anat E Embriol* 82: 157-77, 1977

13, **Tiegs OW.** The nerve net of plain muscle, and its relation to autonomic rhythmic movements. *Austr J Exp Biol Med Sci* 2: 157-166, 1925

14, **Maeda H, Yamagata A, Nishikawa S, Yoshinga K, Kobayashi S, Nishi K, Nishikawa, S-I.** Requirement of c-kit for development of intestinal pacemaker system. *Development* 116: 369-75, 1992

15, **Huizinga JD, Thuneberg L, Kluppel M, Malysz J, Mikkelsen HB, and Bernstein A.** W/kit gene required for interstitial cells of Cajal and for intestinal pacemaker activity. *Nature* 373: 347–349. 1995

16, **Torihashi S, Ward SM, Nishikawa SI, Nishi K, Kobayashi S, and Sanders KM.** c-kit-dependent development of interstitial cells and electrical activity in the murine gastrointestinal tract. *Cell Tissue Res* 280: 97–111, 1995

17, **Ward SM, Burns AJ, Torihashi S, and Sanders KM.** Mutation of the proto-oncogene c-*kit* blocks development of interstitial cells and electrical rhythmicity in murine intestine. *J Physiol (Lond)* 480: 91–97, 1994

18, **Young HM, Ciampoli D, Southwell BR, Newgreen DF.** Origin of interstitial cells of Cajal in the mouse intestine. *Dev Biol* 180: 97-107, 1996

19, **Sanders KM, Torihashi S, Ordog T, Koh SD, and Ward SM.** Development and plasticity of interstitial cells of Cajal. *Neurogastroenterol Motil* 11: 311–338, 1999

20, **Rumessen JJ.** Ultrastructure of interstitial cells of Cajal at the colonic submuscular border in patients with ulcerative colitis. *Gastroenterology* 111: 1447–1455, 1996

21, **Hagger R, Finlayson C, Kahn F, De Oliveira R, Chimelli L, Kumar D**. A deficiency of interstitial cells of Cajal (ICC) in chagasic megacolon. *Gastroenterology* 114: A758–59, 1998 (Abstract)

22, **Vanderwinden J-M and Rumessen JJ.** Interstitial cells of Cajal in human gut and gastrointestinal disease. *Microsc Res Tech* 1; 47: 344-60, 1999

23, **Miettinen M, Sobin LH and Lasota J.** Gastrointestinal Stromal Tumors of the Stomach A Clinicopathologic, Immunohistochemical, and Molecular Genetic Study of 1765 Cases With Long-term Follow-up *Am J Surg Pathol* 29: 52–68, 2005

24, **Paulhe F, Imhof BA, Wehrle-Haller B.** A specific endoplasmic reticulum export signal drives transport of stem cell factor (Kitl) to the cell surface. *J Biol Chem* 279: 55545–55555, 2004

25, **He C-L, Soffer EE, Ferris CD, Walsh RM, Szurszewski JH, Farrugia G.** Loss of interstitial cells of Cajal and inhibitory innervation in insulin-dependent diabetes. *Gastroenterology* 121: 427–434, 2001

26, **Nakahara M, Isozaki K, Hirota S, Vanderwinden J-M, Takakura R, Kinoshita K, Miyagawa J-I, Chen H, Miyazaki Y, Kiyohara T, Shinomura Y, Matsuzawa Y.** Deficiency of KIT-positive cells in the colon of patients with diabetes mellitus. *Journal of Gastroenterology and Hepatology* 17: 666–670, 2002

27, **Burns AJ, Lomax AEJ, Torihashi S, Sanders KM, and Ward SM.** Interstitial cells of Cajal mediate inhibitory neurotransmission in the stomach. *Proc Natl Acad Sci USA* 93: 12008–12013, 1996

28, **Ward SM, Burns AJ, Torihashi S, Harney SC, and Sanders KM.** Impaired development of interstitial cells and intestinal electrical rhytmycity in steel mutants. *Am J Physiol Cell Physiol* 269: C1577–C1585, 1995

29, **Sanders KM, Ördög T, Koh SD, and Ward SM.** A novel pacemaker mechanism drives gastrointestinal rhythmicity. *News Physiol Sci* 15: 291–298, 2000

30, **Ward SM, Ördög T, Koh SD, Abu Baker S, Jun JY, Amberg G, Monaghan K, and Sanders KM.** Pacemaking in interstitial cells of Cajal depends upon calcium handling by endoplasmic reticulum and mitochondria. *J Physiol* 525: 355–361, 2000

31, **Koh SD, Jun JY, Kim TW, and Sanders KM.** A Ca^{2+}-inhibited non-selective cation conductance contributes to pacemaker currents in mouse interstitial cells of Cajal. *J Physiol* 540: 803–814, 2002

32, **Huizinga JD, Zhu Y, Ye J, and Molleman A.** High-conductance chloride channels generate pacemaker currents in interstitial cells of Cajal. *Gastroenterology* 123: 1627–1636, 2002

33, **Tokutomi N, Maeda H, Tokutomi Y, Sato D, Sugita M, Nishikawa S, Nishikawa S-I, Nakao J, Imamura T, and Nishi K.** Rhythmic Cl^- current and physiological roles of the intestinal c-*kit*-positive cells. *Pflügers Arch* 431: 169–177, 1995

34, **Dickens EJ, Hirst GDS, and Tomita T.** Identification of rhythmically active cells in guinea-pig stomach. *J Physiol (Lond)* 514: 515–531, 1999

35, **Sanders KM, Koh SD, Ward SM.** Interstitial cells of Cajal as pacemakers in the gastrointestinal tract. *Annu Rev Physiol* 68: 307–43, 2006

36, **Ward SM, Morris G, Reese L, Wang X-Y, Sanders KM** Interstitial cells of Cajal mediate enteric inhibitory neurotransmission in the lower esophageal and pyloric sphincters. *Gastroenterology* 115: 314 –329, 1998

37, **Indireshkumar K, Brasseur JG, Faas H, Hebbard GS, Kunz P, Dent J, Feinle C, Li M, Boesiger P, Fried M, Schwizer W** Relative contributions of "pressure pump" and "peristaltic pump" to gastric emptying. *Am J Physiol Gastrointest Liver Physiol* 278: G604–G616, 2000

38, **Fox EA, Phillips RJ, Byerly MS, Baronowsky EA, Chi MM, Powley TL.** Selective loss of vagal intramuscular mechanoreceptors in mice mutant for steel factor, the c-Kit receptor ligand. *Anat Embryol* 205: 325 –342, 2002

39, **Ward SM, Beckett EAH, Wang XY, Baker F, Khoyi M, and Sanders KM.** Interstitial cells of Cajal mediate cholinergic neurotransmission from enteric motor neurons. *J Neurosci* 20: 1393–1403, 2000

40, **Sanders KM.** A case for interstitial cells of Cajal as pacemakers and mediators of neurotransmission in the gastrointestinal tract. *Gastroenterology* 111: 492–515, 1996

41, **Sanders KM, Ward SM.** Kit mutants and gastrointestinal physiology. *J Physiol* 578: 33-42, 2007

42, **de Lorijn F, de Jonge WJ, Wedel T, Vanderwinden JM, Benninga MA, Boeckxstaens GE.** Interstitial cells of Cajal are involved in the afferent limb of the rectoanal inhibitory reflex. *Gut* 54: 1107–13, 2005

43, **Fox EA, Phillips RJ, Byerly MS, Baronowsky EA, Chi MM, Powley TL.** Selective loss of vagal intramuscular mechanoreceptors in mice mutant for steel factor, the c-Kit receptor ligand. *Anat Embryol (Berl)* 205: 325–42, 2002

44, **Kraichely RE, Farrugia G.** Mechanosensitive ion channels in interstitial cells of Cajal and smooth muscle of the gastrointestinal tract. *Neurogastroenterol Motil* 19: 245–52, 2007

45, **Camilleri M.** Advances in diabetic gastroparesis. *Rev Gastroenterol Disord* 2: 47–56, 2002

46, **Koch KL.** Diabetic gastropathy: gastric neuromuscular dysfunction in diabetes mellitus: a review of symptoms, pathophysiology, and treatment. *Dig Dis Sci* 44: 1061 – 1075, 1999

47, **Owyang C, Hasler WL.** Physiology and pathophysiology of the interstitial cells of Cajal: from bench to bedside VI. Pathogenesis and therapeutic approaches to human gastric dysrhythmias. *Am J Physiol Gastrointest Liver Physiol* 283: G8 –G15, 2002

48, **Takahashi T, Owyang C.** Vagal control of nitric oxide and vasoactive intestinal polypeptide release in the regulation of gastric relaxation in rat. *J Physiol* 484: 481–492, 1995

49, **Shah V, Lyford G, Gores G, Farrugia G.** Nitric oxide in gastrointestinal health and disease. *Gastroenterology* 126: 903–913, 2004

50, **Mashimo H, Kjellin A, Goyal RK.** Gastric stasis in neuronal nitric oxide synthase-deficient knockout mice. *Gastroenterology* 119: 766–773, 2000

51, **Anvari M, Paterson CA, Daniel EE.** Role of nitric oxide mechanisms in control of pyloric motility and transpyloric flow of liquids in conscious dogs. *Dig Dis Sci* 43: 506–512, 1998

52, **Orihata M and Sarna SK**. Inhibition of nitric oxide synthase delays gastric emptying of solid meals. *J Pharmacol Exp Ther* 271: 660–670, 1994

53. **Ördög T, Takayama I, Cheung WKT, Ward SM, and Sanders KM.** Remodeling of networks of interstitial cells of Cajal in a murine model of diabetic gastroparesis. *Diabetes* 49: 1731–1739, 2000

54, **Forster J, Damjanov I, Lin Z, Sarosiek I, Wetzel P, McCallum RW**. Absence of the interstitial cells of Cajal in patients with gastroparesis and correlation with clinical findings. *J Gastrointest Surg* 9: 102–108, 2005

55, **Lin Z, Forster J, Sarosiek I, Damjanov J, McCallum RW.** Baseline status of interstitial cells of Cajal predicts long-term symptom improvement in gastroparetic patients treated with gastric electrical stimulation *Gastroenterology* 126 (Suppl. 2): A-73, 2004 (Abstract).

56, **Ördög T, Baldo M, Danko R, and Sanders KM.** Plasticity of electrical pacemaking by interstitial cells of Cajal and gastric dysrhythmias in *W/W^{V}* mutant mice. *Gastroenterology* 123: 2028–2040, 2002

57, **Ördög T, Ward SM, Sanders KM.** Interstitial cells of Cajal generate electrical slow waves in the murine stomach. *J Physiol (Lond)* 518: 257–269, 1999

58, **Kong M-F, Horowitz M** Gastric emptying in diabetes mellitus: relationship to blood-glucose control. *Clin Geriatr Med* 15: 321 –338, 1999

59, **Nishikawa T, Edelstein D, Du XL, Yamagishi SI, Matsumura T, Kaneda Y, Yorek MA, Beebe D, Oates PJ, Hammes HP, Giardino I, Brownlee M** Normalizing mitochondrial superoxide production blocks three pathways of hyperglycaemic damage. *Nature* 404: 787–790, 2000

60, **Hribal ML, Oriente F, Accili D.** Mouse models of insulin resistance. *Am J Physiol Endocrinol Metab* 282: E977–E981, 2002

61, **Sima AAF, Li ZG, Zhang W.** The insulin-like growth factor system and neurological complications in diabetes. *Exp Diabesity Res* 4: 235 –256, 2003

62, **Watkins CC, Sawa A, Jaffrey S, Blackshaw S, Barrow RK, Snyder SH, Ferris CD**. Insulin restores neuronal nitric oxide synthase expression and function that is lost in diabetic gastropathy. *J Clin Invest* 106: 373–384, 2000

63, **Takahashi T, Kojima Y, Tsunoda Y, Beyer LA, Kamijo M, Sima AA, Owyang C.** Impaired intracellular signal transduction in gastric smooth muscle of diabetic BB/W rats. *Am J Physiol* 270: G411–G417, 1996

64, **James AN, Ryan JP, Crowell MD, Parkman HP.** Regional gastric contractility alterations in a diabetic gastroparesis mouse model: effects of cholinergic and serotoninergic stimulation. *Am J Physiol Gastrointest Liver Physiol* 287: G612–G619 (2004)

65, **Jackson MW, Gordon TP, SWaterman SA.** (2004) Disruption of intestinal motility by a calcium channel-stimulating autoantibody in type 1 diabetes. *Gastroenterology* 126: 819–828, 2004.

66, **Smith MJ and Koch GL.** Differential expression of murine macrophage surface glycoprotein antigens in intracellular membranes. *J Cell Sci* 87: 113–119, 1987

67, **Ördög T, Redelman D, Horváth VJ, Miller LJ, Horowitz B, Sanders KM.** Quantitative analysis by flow cytometry of interstitial cells of Cajal, pacemakers and mediators of neurotransmission in the gastrointestinal tract. *Cytometry A* 62: 139–149, 2004

68, **Burmester T, Ebner B, Weich B, and Hankeln T.** Cytoglobin: a novel globin type ubiquitously expressed in vertebrate tissues. *Mol Biol Evol* 19: 416–421, 2002

69, **Ördög T, Redelman D, Miller LJ, Horváth VJ, Zhong Q, Almeida-Porada G, Zanjani ED, Horowitz B, Sanders KM.** Purification of interstitial cells of Cajal by fluorescence-activated cell sorting. *Am J Physiol Cell Physiol* 286: C448–C456, 2004

70, **Ward SM, Sanders KM.** Interstitial cells of Cajal: primary targets of enteric motor innervation. *Anat Rec* 262: 125–135, 2001

71, **Beckett EAH, Horiguchi K, Khoyi M, Sanders KM, Ward SM.** Loss of enteric motor neurotransmission in the gastric fundus of Sl/Sl*d* mice. *J Physiol (Lond)* 543: 871–887, 2002

72, **Torihashi S, Yoshida H, Nishikawa S, Kunisada T, Sanders KM.** Enteric neurons express Steel factor-lacZ transgene in the murine gastrointestinal tract. *Brain Res* 738: 323–328, 1996

73, **Ward SM, Ördög T, Bayguinov JR, Horowitz B, Epperson A, Shen L, Westphal H, Sanders KM.** Development of interstitial cells of Cajal and pacemaking in mice lacking enteric nerves. *Gastroenterology* 117: 584–594, 1999

74, **Wu JJ, Rothman TP, Gershon MD.** Development of the interstitial cells of Cajal: origin, Kit dependence and neuronal and nonneuronal sources of Kit ligand. *J Neurosci Res* 59: 384-401, 2000

75, **Russell JW, Sullivan KA, Windebank AJ, Herrmann DN, Feldman EL.** Neurons undergo apoptosis in animal and cell culture models of diabetes. *Neurobiol Dis* 6: 347 – 363, 1999

76, **Seo SY, Kim EY, Kim H, Gwag BJ**. Neuroprotective effect of high glucose against NMDA, free radical, and oxygen-glucose deprivation through enhanced mitochondrial potentials. *J Neurosci* 19: 8849 –8855, 1999

77, **Liu W, Schoenkerman A, Lowe WL Jr**. Activation of members of the mitogen-activated protein kinase family by glucose in endothelial cells. *Am J Physiol Endocrinol Metab* 279: E782 –E790, 2000

78, **Ward SM, Harney SC, Bayguinov JR, McLaren GJ, Sanders KM**. Development of electrical rhythmicity in the murine gastrointestinal tract is specifically encoded in the tunica muscularis. *J Physiol (Lond)* 505: 241 –258, 1997

79, **Horner MJ, Ward SM, Gerthoffer WT, Sanders KM, Horowitz B.** Maintenance of morphology and function of canine proximal colon smooth muscle in organ culture. *Am J Physiol Gastrointest Liver Physiol* 272: G669–G680, 1997

80, **Pandini G, Frasca F, Mineo R, Sciacca L, Vigneri R, Belfiore A.** Insulin/insulin-like growth factor I hybrid receptors have different biological characteristics depending on the insulin receptor isoform involved. *J Biol Chem* 277: 39684 –39695, 2002

81, **Seki K, Komuro T.** Distribution of interstitial cells of Cajal and gap junction protein, Cx 43 in the stomach of wild-type and *W/Wv* mutant mice. *Anat Embryol* 206: 57–65, 2002

82, **Nocka K, Tan JC, Chiu E, Chu TY, Ray P, Traktman P, Besmer P.** Molecular bases of dominant negative and loss of function mutations at the murine c-kit/white spotting locus: W37, Wv, W41 and W. *EMBO J* 9: 1805–1813, 1990

83, **Rich A, Miller SM, Gibbons SJ, Malysz J, Szurszewski JH, Farrugia G.** Local presentation of Steel factor increases expression of c-kit immunoreactive interstitial cells of Cajal in culture. *Am J Physiol Gastrointest Liver Physiol* 284: G313–G320, 2003

84, **Huizinga JD, Berezin I, Sircar K, Hewlett B, Donnelly G, Bercik P, Ross C, Algoufi T, Fitzgerald P, Der T, Riddell RH, Collins SM, Jacobson K.** Development of interstitial cells of Cajal in a fullterm infant without an enteric nervous system. *Gastroenterology* 120: 561–567, 2001

85, **Epperson A, Hatton WJ, Callaghan B, Doherty P, Walker RL, Sanders KM, Ward SM, Horowitz B.** Molecular markers expressed in cultured and freshly isolated interstitial cells of Cajal. *Am J Physiol Cell Physiol* 279: C529–C539, 2000

86, **Takahashi T, Nakamura K, Itoh H, Sima AAF, Owyang C.** Impaired expression of nitric oxide synthase in the gastric myenteric plexus of spontaneously diabetic rats. *Gastroenterology* 113: 1535–1544, 1997

87, **Ejskjaer NT, Bradley JL, Buxton-Thomas MS, Edmonds ME, Howard ER, Purewal T, Thomas PK, Watkins PJ.** Novel surgical treatment and gastric pathology in diabetic gastroparesis. *Diabet Med* 16: 488–495, 1999

88, **Duchen LW, Anjorin A, Watkins PJ, Mackay JD.** Pathology of autonomic neuropathy in diabetes mellitus. *Ann Intern Med* 92: 301–303, 1980

89, **Moscoso GJ, Driver M, Guy RJ.** A form of necrobiosis and atrophy of smooth muscle in diabetic gastric autonomic neuropathy. *Pathol Res Pract* 181: 188–194, 1986.

90, **Kuemmerle JF.** IGF-I elicits growth of human intestinal smooth muscle cells by activation of PI3K, PDK-1, and p70S6 kinase. *Am J Physiol Gastrointest Liver Physiol* 284: G411– G422, 2003.

91, **Kuemmerle JF.** Endogenous IGF-I protects human intestinal smooth muscle cells from apoptosis by regulation of GSK-3β activity. *Am J Physiol Gastrointest Liver Physiol* 288: G101–G110, 2005

92, **Bertrand F, Desbois-Mouthon C, Cadoret A, Prunier C, Robin H, Capeau J, Atfi A, Cherqui G.** Insulin antiapoptotic signaling involves insulin activation of the nuclear factor κB-dependent survival genes encoding tumor necrosis factor receptor-associated factor 2 and manganese-superoxide dismutase. *J Biol Chem* 274: 30596–30602, 1999

93, **Hsueh WA, Law RE.** Insulin signaling in the arterial wall. *Am J Cardiol* 84: 21J–24J, 1999

94, **Feldstein AE, Miller SM, El-Youssef M, Rodeberg D, Lindor NM, Burgart LJ, Szurszewski JH, Farrugia G.** Chronic intestinal pseudoobstruction associated with altered interstitial cells of Cajal networks. *J Pediatr Gastroenterol Nutr* 36: 492– 497, 2003.

95, **Chang I-Y, Glasgow NJ, Takayama I, Horiguchi K, Sanders KM, Ward SM.** Loss of interstitial cells of Cajal and development of electrical dysfunction in murine small bowel obstruction. *J Physiol (Lond)* 536: 555–568, 2001

96, **Flohé SB, Wasmuth HE, Kerad B, Beales PE, Pozzilli P, Elliott RB, Hill JP, Scott FW, Kolb H.** A wheat-based, diabetes-promoting diet induces a Th1-type cytokine bias in the gut of NOD mice. *Cytokine* 21: 149–154, 2003.

97, **Parkman HP, Hasler WL, Fisher RE.** American Gastroenterological Association echnical review on the diagnosis and treatment of gastroparesis. *Gastroenterology* 127: 1592–1622, 2004

98, **Soler NG.** Diabetic gastroparesis without autonomic neuropathy. *Diabetes Care* 3: 200–201, 1980

99, **Clouse RE, Lustman PJ.** Gastrointestinal symptoms in diabetic patients: lack of association with neuropathy. *Am J Gastroenterol* 84: 868–872, 1989.